POLITÉCNICO DE LEIRIA | ESCOLA SUPERIOR DE TURISMO E TECNOLOGIA DO MAR

Biosilica from deep-sea marine sponge Geodia barretti for the development of 3D printed scaffolds for bone tissue regeneration applications

Rodrigo Valente Colares

2021

POLITÉCNICO DE LEIRIA | ESCOLA SUPERIOR DE TURISMO E TECNOLOGIA DO MAR

Biosilica from deep-sea marine sponge Geodia barretti for the development of 3D printed scaffolds for bone tissue regeneration applications

Rodrigo Valente Colares

Dissertation Report to obtain the Master's Degree in Marine Resources Biotechnology

Dissertation carried out under the guidance of Doctor Tiago Henriques da Silva, Doctor Catarina Marques and Doctor Olesia Dudik and co-supervision of Doctor Clélia Correia Neves Afonso

2021

Title: Biosilica from deep-sea marine sponge Geodia barretti for the development of 3D printed scaffolds for bone tissue regeneration applications.

Agradecimentos

A dissertação de mestrado apresentada é o culminar de um trabalho que só foi exequível graças ao apoio, emprenho, dedicação e sacrifício de inúmeras pessoas que, de um modo ou de outro, tiveram um papel essencial. Por conseguinte, gostaria de agradecer:

Ao Doutor Tiago Silva, orientador científico desta tese, e à Doutora Catarina Marques e Doutora Olesia Dudik, que acompanharam de perto todo este trabalho, contribuindo de forma exemplar para minha formação científica. Por toda disponibilidade, apoio, espírito crítico e paciência, o meu muito obrigado!

Ao Professor Doutor Rui Reis, diretor do I3B's Research Group, por permitir que este trabalho de investigação fosse desenvolvido na instituição. Também meu especial obrigado à toda equipa técnica do 3Bs, Doutora Gabriela Diogo, Doutora Eva Martins, Lara Pierantoni e Doutor Ricardo Pires, pela assistência em momentos essenciais para a execução deste trabalho.

À minha Mãe e minha querida Gunta, que por tantas vezes, mesmo que não percebessem "bulhufas" do que eu estava a fazer, estavam sempre a motivar, ser compreensivas, apoiando-me incondicionalmente em todo o percurso e souberam me dar suporte nos momentos que mais precisei.

Aos colegas que pude conhecer na trajetória desta dissertação, em especial ao Eduardo Backes pelos tantos momentos bem-humorados, mas sobretudo pela generosidade ao partilhar conhecimento, hoje posso dizer que é um dos grandes amigos que a tive a felicidade de conhecer. Àqueles que diariamente tornavam a rotina mais leve, em tempos pré-pandemia, nos almoços e cafés, durante o confinamento com muito suporte mental mútuo, e na alegria de se ver no desconfinamento, Eduardo Silva, Margarida, Ângela, Bia e Lya.

Aos colegas que me receberam tão efusivamente na *Library Crew,* e os que chegaram depois no "barquinho" que navegamos juntos, entre alegrias, motivações, companheirismo e alguma "cultura prescindível". Aos colegas de Erasmus com quem tive o prazer de partilhar culturas e conhecimento.

Aos professores da Escola Superior de Turismo e Tecnologia do Mar de Peniche, com quem pude aprender com entusiasmo a base científica em biotecnologia e biologia marinha, que me possibilitou desenvolver esta dissertação, aos que davam motivação contínua para chegar cada vez mais longe e que em muitos momentos fizeram-me sentir

como em casa. À malta da Tuna que me fez viver uma experiência indescritível como estudante em Portugal desde os meus primeiros dias.

Aos amigos de Braga, compadres Taissa e Pedro, a pequena Maya, Gabi, José, Anna, Alexey, Thomaz, Gustavo, aos que mesmo distantes se fazem presentes, minhas primas Tarcila e Taiana e Paulinha, meu irmão do coração Elkjaer, Sarah, e tanta gente boa que conheci nesses anos, que de diversas formas ajudaram-me a manter o espírito aquecido e a alegria presente.

A todos o meu muito obrigado!

ABSTRACT

The oceans have always been a great instigator of human curiosity and, from the time of great navigations to the present day, the source of knowledge seems to be growing. It is estimated that the biodiversity of the oceans is greater than that of tropical forests, being still little known and considered the last barrier to scientific discoveries on the planet. Marine sponges are one of the oldest invertebrate animals in this environment, being studied more recently by several areas of research, mainly for their interaction with other microorganisms and structural properties. Marine sponges present a vast number of bioactive compounds with diverse biological activities, as antitumoral, antibacterial and anti-inflammatory properties, that can be used in therapeutic approaches, namely in regenerative medicine. Additionally, biosilica from marine sponges became attractive for engineers for its application in bone tissue engineering strategies.

The biosilica from Geodia barretti (GB) was a target material in our study compared to Diatomaceous Earth (DE) and Bioglass® 45S5 (BG) in producing alginate-based inks for 3D printing scaffold fabrication. The obtaining of GB based ceramic particles was executed through the calcination process. Prior to ink formulation, production the silica particles from GB, DE and BG were size standardized in the range from 36 to 63 μm and physic-chemically characterized with use of Fourier-transform infrared spectroscopy (FTIR), X-Ray diffraction (XRD) and Scanning electron microscopy - Dispersive X-ray spectroscopy (SEM/EDS). Composite inks were developed by mixture of silica-based materials with alginate solution and the respective rheological evaluation presented stable viscous and elastic moduli, supporting the advance to the 3D-printing for production of scaffolds. The porosity and pore size distribution of the obtained scaffolds were evaluated by X-ray micro-CT imaging technique, showing their high porosity and interconnectivity. Bioactivity of scaffolds was analyzed by immersion into simulated body fluid up to 21 days followed by detection of calcium phosphate formation on their surface, after each time point, using SEM/EDS. Mechanical tests results point to insufficient compression properties when compared to the ones exhibited by the target tissue (human bone). The biological evaluation of silica-alginate scaffolds with and without collagen coating showed that the formulations with GB biosilica were performing equally or better than the others, with the addition of collagen improving the cell adhesion and proliferation in the scaffolds.

Keywords: bone tissue engineering, biosilica, marine biotechnology, 3D-printing

RESUMO

Os oceanos sempre foram um grande instigador da curiosidade humana e, desde os tempos das grandes navegações até os dias atuais. Estima-se que a biodiversidade dos oceanos seja maior do que a das florestas tropicais, sendo ainda pouco conhecida e considerada a última barreira às descobertas científicas no planeta. As esponjas marinhas são um dos animais invertebrados mais antigos neste ambiente, sendo estudadas mais recentemente por várias áreas de investigação, pela sua interação com outros microrganismos e propriedades estruturais. As esponjas marinhas apresentam composições fisiológicas, que podem ser utilizados em abordagens terapêuticas, nomeadamente na medicina regenerativa. Além disso, a biossílica de esponjas marinhas tornou-se atraente por sua aplicação em estratégias de engenharia de tecido ósseo.

A biossílica de Geodia barretti (GB) foi um material alvo em nosso estudo em comparação com Diatomaceous Earth (DE) e Bioglass® 45S5 (BG) na produção de tintas à base de alginato para fabricação de andaimes de impressão 3D. A obtenção das partículas cerâmicas à base de GB foi realizada através do processo de calcinação. Antes da formulação da tinta, a produção das partículas de sílica de GB, DE e BG foram padronizadas por tamanho na faixa de 36 a 63 μm e caracterizadas físico-quimicamente com o uso de espectroscopia de infravermelho por transformada de Fourier (FTIR), difração de raios-X (XRD) e Microscopia Eletrônica de Varredura - Espectroscopia Dispersiva de Raios-X (MEV / EDS). As “tintas” foram desenvolvidas pela mistura de materiais à base de sílica com solução de alginato e a respetiva avaliação reológica apresentou módulos viscosos e elásticos estáveis, apoiando o avanço para a impressão 3D para produção de scaffolds. A porosidade e distribuição de tamanho de poro dos scaffolds obtidos foram avaliados pela técnica de imagem de micro-TC de raios-X, mostrando sua alta porosidade e interconectividade. A bioatividade dos scaffolds foi analisada por imersão em fluido corporal simulado por até 21 dias seguida pela deteção da formação de fosfato de cálcio em sua superfície, usando MEV / EDS. Os resultados dos testes mecânicos apontam para propriedades de compressão insuficientes quando comparadas às exibidas pelo tecido-alvo. A avaliação biológica dos scaffolds de sílica-alginato com e sem recobrimento de colágeno mostrou que as formulações com biossílica GB tiveram desempenho igual ou melhor que as demais, com a adição de colágeno melhorando a adesão e proliferação celular nos scaffolds.

Palavras-chave: engenharia de tecido ósseo, biossílica, biotecnologia marinha, impressão 3D

LIST OF CONTENTS

LIST OF FIGURES

LIST OF TABLES

LIST OF ABBREVIATIONS

µg	Microgram
µL	Microliter
µm	Micrometer
Alg	Sodium alginate
BG	45S5 Bioglass®
BS	Biosilica
COL1	Collagen type I
DE	Diatomaceous earth
DMEM	Dulbecco's Modified Eagle Medium
DNA	Deoxyribonucleic acid
ECM	Extracellullar matrix
EDS	Energy-dispersive X-ray spectroscopy
EO	Ethylene oxide
FBS	Fetal Bovine Serum
FSF	Fossil shell flour
FTIR	Fourier-transform infrared spectroscopy
GB	*Geodia barretti*
GPa	Giga Pascal
M	Unit of molar concentration
mM	Milimolar
mL	Milliliter
mg	Milligram
mm	Millimeter
MPa	Mega Pascal
N	Newton
PBS	Phosphate Buffered Saline
PG	PicoGreen™
rpm	Revolutions per minute
SaOS-2	Sarcoma osteogenic cell line
SEM	Scanning Electron Microscopy
w/v	Weight by volume
wt.	Weight
XRD	X-ray diffraction

1. INTRODUCTION

The oceans cover above 70 percent of Earth's surface and provide about 90 percent of water for the living space on the planet (NOAA, 2021). The ocean biodiversity is still more than 80 percent unexplored and scientists estimate that 91 percent of ocean species have yet to be classified (Mora et al., 2011), which urges mankind inspiration for discovering the extreme environment. It is generally known that oceans provide many unique environments and resources, with diverse marine organisms with great potential for biotechnology research fields (Burgess, 2012; Chinnappan et al., 2015; Kiuru et al., 2014; Montaser & Luesch, 2011).

Besides developing products from a natural deep-sea source for technological purposes, examining marine patterns and processes of ecosystems would also contribute to valorizing the environment and reinforcing sustainable exploitation. Most natural-origin products are composed of bioactive chemical compounds, which with recent advances on what concerns the Research and Technological Development industry, have been isolated and identified (David, Wolfender, & Dias, 2015) (Akabane, 2019) (Ravali, 2011) (Maher, 2013). Many of these compounds are used in conjunction with other compounds, synthetic or natural, for the production of biomaterials[1] in various applications, especially in biomedicine (Alves, 2020; Carvalho et al., 2018; Seixas et al., 2020; Shavandi et al., 2017).

At the same time, the valorization of by-products from marine origin could represent a development of a highly valued product chain (Ivanova et al., 2016). The marine biomaterials from new sources, as well from well-known sources, have been applied in several biotechnological fields, namely biomedicine, from preventive pharmacology to post-surgical therapeutic areas, applying to the treatment of chronic diseases - like cancer, myocarditis, osteoporosis, e.g. - traumas or even tissue and organ replacement (Simmons, Andrianasolo, McPhail, Flatt, & Gerwick, 2005) (Senthilkumar & Kim, 2013) (Lordan, Ross, & Stanton, 2011).

Among marine organisms, marine sponges can produce or metabolize compounds for protection or excretion when in contact with microorganisms, particularly during the filtration process. The marine sponges are the organisms with attributes that attract the researchers' interest due to their potential for biomedical applications (Grassle & Maciolek, 1992; Pallela & Ehrlich, 2016; Perdicaris, Vlachogianni, & Valavanidis, 2013; Suarez-Jimenez, Burgos-Hernandez, & Ezquerra-Brauer, 2012). There are many bioactive

[1] A biomaterial is defined as a substance that has been engineered to interact with biological system for a medical purpose.

compounds in the sponge structure with anti-inflammatory, anticancer, antiviral, antimalarial properties, among others.

Classes Demospongiae, *Hexactinellida*, *and Homoscleromorpha* (Cassarino, Coath, Xavier, & Hendry, 2018) are siliceous sponges, presenting skeleton made up of biosilica. They present interesting mechanical properties, associated to astonishing morphological features, based on their capacity to expand and contract in water and filtrate a large amount of water (Abdelmohsen, Abdelmohsen, Bayer, & Hentschel, 2014) (Sagar, Kaur, Radovanovic, & Bajic, 2013) (Sabdono & Radjasa, 2011) (Woesz, et al., 2006). Besides, they are perfectly adapted to a wide range of ecological aquatic niches and interact with different microorganisms (Hardoim & Costa, 2014) (Sagar, Kaur, & Minneman, Antiviral Lead Compounds from Marine Sponges, 2010) (Silva, Oliveira, Mano, & Reis, 2014).

Species within *Demospongiae* are very diverse and present the subject to continuous study of their distribution in oceans and taxonomy (Cárdenas & Rapp, 2015; Schuster et al., 2021). Besides, they have been also explored from the biotechnological point of view, with some species being considered as inspiration for the development of biomimetic biomaterial for tissue engineering (Martins et al., 2019).

The following sections will briefly describe some relevant characteristics of the *Geodia barretti* sponge of *Demospongiae* Class, marine origin biosilicas and biopolymers used throughout the thesis work.

1.1. Geodia barretti

The *Geodia barretti* (GB) was first described by Bowerbank (1858) (Demospongiae, Geodiidae), and it's found in deep waters. According to Picton et al. (2011), this marine sponge species has a restricted distribution in North Atlantic and the Arctic, commonly in European Marine Waters along the Barents Sea, Denmark Strait, Faroe Islands, and Norwegian coast, especially common in the Scandinavian fjord areas, as noted in Figure 1A. It is described as a large globular smooth sponge with a hard consistency (Klitgaard & Tendal, 2004). The natural color is cream-yellow or pale yellow-white, characterized by one or several deep-sunken openings, which contain groups of exhalant oscules (Figure 1B).

The barettin, a molecule first isolated from *G. barretti* in 1986, presented antioxidant and anti-inflammatory potential as reported in recent studies (Lind et al., 2013) and it was associated with treating diseases that affect the immune system and diseases that are caused by inflammation. Barretin was also related to the inhibition of the settlement of barnacle larvae and acts as an antifouling agent (Bohlin et al., 2010). Besides, several other

compounds have been isolated, characterized and synthesized from *G. barretti*, increasing the interest for this sponge (Carstens et al., 2015).

For the present study, the *Geodia* genus was chosen by the high density of siliceous spicules (Müller, et al., 2007) and the morphology of *Demospongiae*; the GB siliceous spicules' particle morphology can be noted in Figure 1C. To obtain the bioceramics particle from GB, it is important first to remove the organic portion, to enable a more accurate study of the spicule's morphology and chemical composition. The isolation of bioceramics from *Geodia* was described through the calcination process (Dudik et al., 2018) to remove the organic portion.

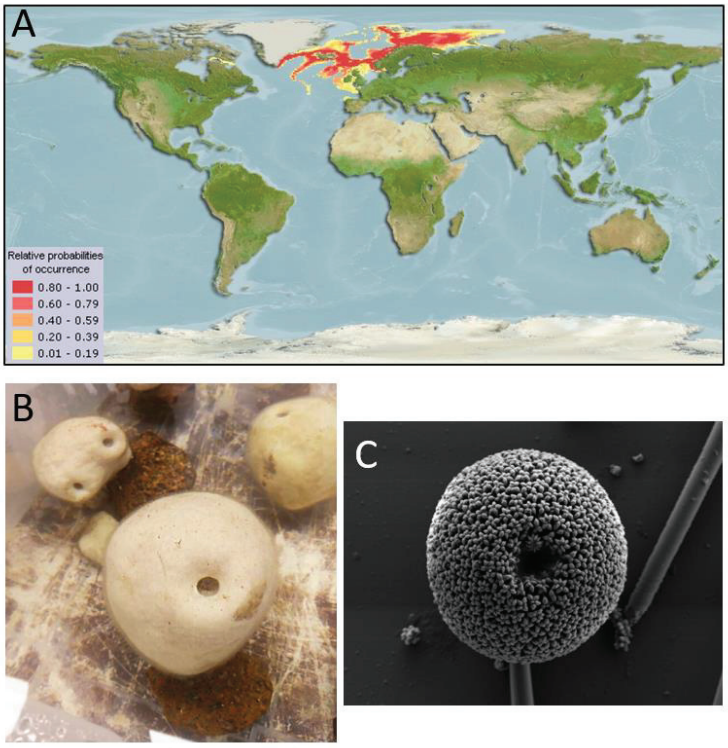

Figure 1. **A** - *Geodia barretti* native range with relative probabilities of occurrence (Adapted from AquaMaps, 2019). **B** –*Geodia barretti* samples (FAO-UN, 2021). **C** - Scanning electronic micrograph of *Geodia barretti*'s microsclere at 1000x magnification (Cárdenas & Rapp, 2015).

1.2. Bioceramics: marine origin biosilica

The bioceramics are an important subset of the biomaterials, which could be natural or artificial, presenting the required biocompatible and non-toxic features, designed to induce a specific biological activity in the target biological system. They can be from non-

degradable to very resorbable and eventually are incorporated or substituted by the body after regeneration assistance.

The natural pathway for bioceramics synthesis occurring in some organisms is called biomineralization, described as the phenomenon which drives the development of biological structures, associating organic matrices to inorganic functional nanostructures phases (Sprio et al., 2014). The inorganic phases are called biominerals, and as a consequence of organism metabolism, they can be deposited in the tissue of these living organisms (Catherine & Skinner, 2000). The biomineralizers can inspire breakthroughs in artificial biomimetic technological advances (Demadis, 2020). Corals and sponges are the common reference for marine biomineralizers. They can provide an abundant source of chemical components depending on the organism, environmental conditions, and interaction with other organisms or microorganisms.

One of the most widespread biogenic minerals is biosilica, which consists of glassy amorphous silica and is formed in many aquatic organisms, plants and grasses. Some of the most representative organisms in this category are sponges and algae (Walsh, 2015). Bioseparation methods to obtain the biosilica from these organisms, mainly purification, are still scarce. Biosilica has interesting properties for the development of innovative therapies for bone pathologies, having bone mineral affinity and morphological similarities as vascularity and porosity (Nandi, et al., 2015). In this perspective, biosilica is widely used for the fabrication of biomimetic and biodegradable biomaterials for bone tissue engineering applications (Ma, 2008) (Nguyen, et al., 2012) (Smith & Ma, 2011) (Venkatesan, Anil, Chalisserry, & Kim, 2016).

The biosilica from marine sponges and diatoms has shown osteogenic potential and affinity with bone minerals, being considered in many studies with biotechnological approaches, namely for manufacturing micro to nano-scale structures for optical systems, but also to drug delivery (Gabbai-Armelin, et al., 2019) (Wiens, et al., 2010) (Müller, Albert, Schröder, & Wang, 2014) (Schröder, Wiens, Wang, Schloßmacher, & Müller, 2011). Regarding bone therapeutic approaches, studies have shown the chemical composition influence over the biological assay using SaOS-2 cell line, a cell line commonly used as model of osteoblasts. Biosilica has also been used in combination with biopolymers, as alginate and collagen, for the development of scaffolds for tissue engineering, with the incorporation of biosilica resulting in a mechanical improvement of the scaffolds in the compressive mode (Lalzawmliana et al., 2019; Xiaohong Wang, Schröder, & Müller, 2014).

Another source of biosilica are diatoms, an important group of microalgae found in the world's oceans, waterways, and soils, which plays a vital role in oxygen production on

Earth (Hildebrand, 2015) and can be used for a variety of purposes, including water filtration and fertilization (Bhardwaj, 2005) (Pati, 2016). The diatoms' cell wall is made of silicon dioxide particles, assembled in a highly organized structure with porous networks at different scales that remain intact when cells die, offering inorganic structures with interesting morphological characteristics for potential research and development applications (Moreno & Fernando, 2015)(Walsh et al., 2017) (Hamm, 2005).

Diatom silica is widely being used for health applications in the delivery of therapeutic agents (Zhang et al., 2013; Aw et al., 2013; Losic et al., 2010) and as fillers to match bone defects (Plazas et al., 2014). The studies by Cicco et al. and Vona et al. revealed that diatom silica can be used as a multifunctional smart material for bone cell growth-promoting tissue regeneration (Vona et al., 2016).

Within the last 20 years in biomedical research, considerable interest has been generated regarding silica/biosilica particles for their potential to possess important characteristics, for example, high biocompatibility; stability and easy internalization; high traceability and imaging capacity; low toxicity; and specificity (Bharti et al., 2015; Kankala et al., 2020; Pham et al., 2021; Vivero-Escoto et al., 2012).

1.3. Biopolymer

Biopolymers are natural polymers produced by the cells of a living organism, which consist of monomeric units that are covalently bonded to form larger molecules. The main biopolymers are in three groups: polynucleotides, polypeptides, and polysaccharides, classified according to the monomer used in the structure; besides, there are some biopolymers out of these groups, as suberin, melanin or latex. The biopolymers have applications in many fields of industry, i.e., food industry, manufacturing, and biomedical engineering (Kim et al., 2010; Kumar et al., 2012; Scholten et al., 2014; Senior et al., 2019; Walsh et al., 2017).

One of the main purposes of biomedical engineering is to fabricate biomaterial, which will rebuild new tissue and be integrated into neighboring tissues to restore normal body functions. Many natural-origin polymers can be used for regenerative medicine, tissue engineering, drug delivery, and medical device development due to their biocompatibility, non-toxicity, biodegradability, mechanical properties, and stability (Araujo et al., 2012; Kozlowska et al., 2018; Naleway et al., 2016; Verdugo, 2007).

Marine organisms provide a rich source of chemically diverse compounds. For instance, the bioactive and highly branched sulfated polysaccharide fucoidan and the anionic polysaccharide alginate can be extracted from brown algae and are used as

scaffolding materials for bone and cartilage tissue regeneration (Z. Li & Zhang, 2005; Pajovich & Banerjee, 2017). Additionally, collagen has been isolated from several fish species, including codfish, as well as from jellyfish and other marine invertebrates, being proposed to be used in biomaterials for bone and cartilage regeneration (Addad et al., 2011; Hoyer et al., 2014; Kozlowska et al., 2018; Oliveira et al., 2021).

Alginate

Alginate is found in brown algae cell walls building up to 45% of the dry weight of these seaweeds. It is an abundant marine biopolymer and has been extracted from different seaweed species, as *Macrocystis pyrifera*, *Ascophyllum nodosum*, and types of *Laminaria*. This natural polymer is composed of linear copolymers of 1β-d-mannuronic acid and α-l-guluronic acid and presents the chemical formula $(C_6H_8O_6)_n$. It is hydrophilic and possesses elastic properties (Lee & Mooney, 2012). It has weak mechanical strength, that could be improved during biomaterial preparation for enhanced mechanical and structural functions applications.

The first application of alginate was in the form of a dressing when its gelation and absorbent properties were discovered (Paul & Sharma, 2015). When applied to wounds, alginate produces a protective gel layer ideal for tissue healing and regeneration while maintaining a stable temperature environment. Alginate is a widespread ingredient for health-related preparations, from dentistry to additive manufacturing. It can be used as a material for microencapsulation, medical devices, and tissue regeneration. One of the most used forms of alginate hydrogel is that when cross-linked with calcium ions (Hernández-González et al., 2020).

The alginate hydrogel is a biologically inert material widely used to fabricate scaffolds, especially in extrusion-based printing (Wu, et al., 2016). These hydrogels have the characteristic to mimic the extracellular matrix (Sargus-Patino, 2013) (Rowley, Madlambayan, & Mooney, 1999). Besides, the versatility of this material, porosity structure, and soft nature allows the nutrient and oxygen diffusion into products (Sarker, et al., 2014) (Donati & Paoletti, 2009) (Augst, Kong, & Mooney, 2006). According to study by Hernández-González et al., "*alginate hydrogels are one of the most assayed hydrogels for 3D Printing and bone tissue engineering and bioprinting due to their properties such as gelling capacity, low toxicity, and low cost*" (Hernández-González, Téllez-Jurado, & Rodríguez-Lorenzo, 2020).

Collagen

Collagen is the main structural protein in the extracellular matrix, an essential component of the conjunctive tissue, and the most abundant protein in mammals – 25% to 35% of the whole-body protein content. It consists of three alpha chains of amino acids that are organized in the form of a triple helix, also known as a collagen helix (Ramshaw et al., 2009). There are up to 28 types of collagens identified in the human organism, but collagen type I (COL1) is over 90% in the human body (Ricard-Blum, 2011). The collagen deficiency is called collagenosis, resulting in poor bone formation, muscle stiffness, growth problems, inflammation in muscle joints, skin diseases (Wolff, 2007).

The most common motifs in the amino acid sequence of collagen are glycine-proline-X and glycine-X-hydroxyproline, where X could be any amino acid other than glycine, proline, or hydroxyproline, being the latter characteristic of these proteins. Other amino acids commonly found in mammals' or fishes' skins are alanine, glutamic acid, arginine, aspartic acid, serine, lysine, leucine, valine, threonine, and others in lower concentrations (Shoulders & Raines, 2009).

Collagen can be used for a wide variety of applications, from the food industry to medicine (Irastorza et al., 2021). The main source of collagen is bovine and porcine skin, but many studies have been carried out to extract collagen from marine sources (Subhan et al., 2015). It is important to find alternative sources of collagen, given the unpopular use of collagen from pig or cow skins due to religious restrictions and the active discussion about the use of bovine collagen due to mad cow disease and the risk they represent for humans (Dayton, 2008; Silva et al., 2014). Additionally, the collagen from marine origin has shown unique advantages compared to collagens extracted from the conjunctive tissue of mammals, as a lower known risk of transmission to humans of infections-causing agents and it is from a source far less associated with cultural and religious concerns. (Silva et al., 2014)

Techniques to obtain collagen from marine sources have been developed considering different organisms – fishes, sponges, jellyfishes, e.g. –, resulting in materials with several physicochemical properties that could be applied in products as compact or very long fibers, films, micro or nanoparticles, or porous scaffolds for biomimetically inspired hybrid materials or biocomposites (Gomez-Guillen et al., 2011). The potential of materials obtained from industry by-products (adding to their value chain and preventing their waste), as well as the properties of various marine-based biomaterials, is drawing the attention of the scientific community.

According to Ghorbania *et al.*, collagen has been used to develop bone substitutes "*owing to hydrophilicity, biodegradability, and potential for simulation of natural tissue component*" (Ghorbani et al., 2020). The biofunctional molecules in their chemical structure are responsible for important properties in the bone tissue substitutive material component (Sahranavard et al., 2020).

The COL1 was chosen for this study due to its advantages for scaffolds fabrication in bone tissue engineering, such as osteogenic differentiation enhancement, the presence of cell recognition and adhesion sites, biocompatibility, bioresorbability – natural absorbing, or biodegradability – and non-toxicity (Chiu et al., 2014; Akhir & Teoh, 2020).

1.4. Bone tissue engineering applications

Bone is the second most transplanted tissue (Shegarfi & Reikeras, 2009; Williams & Szabo, 2004), losing only for blood transfusions, and alongside cartilage, has the most replication attempts described. The most frequent causes of bone replacement are accidents, cancer, deficiency in bone formation, diabetes amputation cases, correction surgeries, and other diseases affecting bone integrity related to population aging, like osteoporosis and mineral loss (Patients et al., 2012; Stein, Ebeling, & Shane, 2007; Weisinger, Carlini, Rojas, & Bellorin-Font, 2006). A bone substitute material must mimic the bone functions, such as morphology, bone formation ability - mineralization, degradability, mineral composition, porosity, biocompatibility (Kampleitner, Obi, Vassilev, Epstein, & Hoffmann, 2018). However, the complexity of bone tissue makes it challenging to mimic and, until now, no material has been described that can simultaneously fulfill all these requirements (Sheikh et al., 2015; Greenwald, et al., 2001; Roberts & Rosenbaum, 2012). Different approaches have been attempted, whether natural products, synthetics, composites, or even these materials containing living cells and a recent study suggested that commercial biosilica or bioactive glasses seem relevant for bone tissue engineering applications (Özarslan et al., 2021) and new sources may reduce production cost of these materials.

Marine biotechnology enables the exploration of an almost infinite material source for biomedical applications, promising a good cost-benefit ratio and sustainable processes, thus representing a potential increment for the green economy (Buonocore, 2012). In this perspective and as addressed above, marine organisms can be studies as source of biosilica-based materials and the deep-sea marine sponge *Geodia barretti* can be evaluated

as an interesting biosilica source using the full organic removal process, as recently described (Dudik, O. 2021).

Together with calcium phosphates (CaPs), bioactive glasses (BGs) have been whidely explored for dental and orthopedic applications (Paez et al., 2018; Thomas, S., Balakrishnan, P., & Sadasivan, 2018). Bioactive glasses are a synthetic silica-based material, defined as glass-ceramic, composed of microcrystals dispersed in glass-liquid transition, with biocompatibility and bioactivity properties, promoting interaction to the biological system by forming a strong material tissue bond. The term “Bioglass” was trademarked by the University of Florida and is first referred to the original 45S5 composition proposed by Larry Hench in 1969, based upon his theory of the body rejecting metallic or polymeric materials unless it was able to form a coating of hydroxyapatite which is found in bone. After Hench's discovery, many variations were proposed, as S53P4, 58S or 70S30C, with the name commonly being a reference to the chemical formula composition: 45S5 is composed by 45 wt. % of SiO_2 and 5:1 molar ratio of Calcium to Phosphorus, S53P4 presents 53 wt. % of SiO_2 and 4 wt. % of P_2O_5, 58S presents 58 wt. % of SiO_2, 70S30C presents 70 wt. % of SiO_2 and 30 wt. % of CaO. These different compositions were proposed for different applications of biological systems, such as small implants in non-load bearing applications, bone filler and scaffolds to promote new bone tissue formation.

The first clinical experiments using bioglasses occurred during the 1980s to middle 1990s decades, with significant assays being thus performed fifteen years later the first BioGlass 45S5 synthesis. A bioactive glass was successfully implanted in animals in 1986, and it was the first material to be able to create strong bonds with living bone tissue, described with chemical and mechanical resistance and firm intergrowth. Nowadays the BG 45S5 is regarded as the gold standard in bone regenerative repair (Gorustovich et al., 2010; Hench, 1998; Türe, 2019).

Three-dimensional (3D) printing

Over the last several decades, researchers have developed different kinds of scaffolds for bone tissue regeneration (Gao et al., 2014; Ge et al., 2008; Gusić et al., 2014; Pilia et al., 2013). Each of the scaffolding strategies employed has its advantages and disadvantages, which define their effectiveness. Successful strategy translation is restricted by practical requirements, i.e. ease and reproducibility of fabrication, stability, choice of bioactive materials, and by satisfying the structural, mechanical, and biological requirements for the bone repair with satisfactory long-term outcomes (J. J. Li et al., 2014).

Additive manufacturing, particularly 3D printing, is an engineering technique

becoming more popular in biomaterials science over the years (Groll et al., 2016), fabricating scaffolds, orthoses, and prosthetic devices for tissue engineering applications (Pugliese et al., 2021). The 3D printing techniques have been modulated to develop tissue engineering materials and their popularity has been increased with recent advances, as the control to generate customized and patient-specific constructs, and development of new technologies for equipment (Bose, Vahabzadeh, & Bandyopadhyay, 2013) (Mistry, 2018) (Sinha, 2020). Nevertheless, the development of printing materials – inks – is a challenge given the need to combine printability (associated with certain rheological properties) with properties related with biological performance, namely optimizing cell adhesion, proliferation towards new tissue formation (Khan, Yaszemski, Mikos, & Laurencin, 2008). According to the design, some of the characteristics for a good 3D-printing performance are the ink material flow and 3D modeling formation, precise placing the cells, recreating a 3D niche with ink materials that overcomes defects of 2D structures (Groll et al., 2016). The printable biomaterial ink should have the inducing particles to facilitate the dispersion of the cells in the scaffold during the cell seeding (Melchels et al., 2010). For the biological evaluation, the material should have good water absorption, and the material must have a good adaption in the human body, with replacement of the target tissue (Melchels et al., 2010).

Alginates form gels in the presence of divalent ions (typically Ca^{2+}, Sr^{2+} or Ba^{2+}) at physiological conditions, providing great versatility in gelation strategies for *in situ* formations of hydrogel networks, as well as higher-order structures, making them quite attractive for bioprinting strategies (Pataky et al., 2012) from which the combination of alginate with collagen could improve the performance of the resulting mixture. This combination will not affect the capacity of the mixture to support mineralization due to the high calcium affinity of alginate (Xie et al., 2010).

Biosilica and collagen present properties of interest for tissue engineering and three-dimensional techniques and when associated with other materials, or biomaterials, can optimize their applications, for example with metals or incorporation in hydrogels, which can increase the durability and resistance of the devices. From literature data, it can be concluded that silica-based materials are excellent candidates to be used as starting materials for the manufacture of 3D scaffolds for bone tissue engineering (Madhumathi et al., 2009; Nejati, 2015; Nommeots-Nomm et al., 2017; Özarslan & Yücel, 2016; Sowjanya et al., 2013; Xiaohong Wang, Tolba, et al., 2014).

1.5. Objectives

The main goal of the present work was to develop marine origin biosilica-based porous scaffolds by 3D printing, using the deep-sea marine sponge *Geodia barretti* as a biosilica source, and further to evaluate their physicochemical and biological properties. To evaluate their potential for bone tissue engineering applications the scaffolds were compared with fabricated scaffolds based on Diatomaceous earth biosilica (another type of biosilica) and Bioglass 45S5® (a synthetic silica-based material, the gold standard of this type of materials).

The global aims of the work can be broken down in 6 specific objectives:

1. Bioseparation of biosilica (BS) from *Geodia barretti* and determine the biosilica component under laboratory conditions;
2. Physicochemical characterization of silica particles (Diatomaceous earth - DE; Bioglass 45S5® - BG; Biosilica from Geodia barretti – GB);
3. Development of ink formulations based on silica particles and alginate hydrogel, and evaluation of their properties for 3D printing;
4. Production of silica-based scaffolds by 3D printing;
5. Physicochemical characterization of 3D printed scaffolds;
6. *In vitro* biological assessment of the developed scaffolds.

Development of 3D printed scaffolds based on biosilica from deep-sea marine sponge *Geodia barretti* for bone tissue regeneration strategies

R. V. Colares[1,2], O. Dudik[1, 2], C. F Marques[1, 2], G. Diogo[1, 2], E. Martins[1, 2], R. A. Pires [1, 2], R. L. Reis[1, 2], T. H, Silva[1, 2]

[1]3B's Research Group, I3Bs – Research Institute on Biomaterials, Biodegradables and Biomimetics, University of Minho, Headquarters of the European Institute of Excellence on Tissue Engineering and Regenerative Medicine, AvePark, Parque de Ciência e Tecnologia, Zona Industrial da Gandra, 4805-017 Barco, Guimarães, Portugal

[2]ICVS/3B's – PT Government Associate Laboratory, Braga/Guimarães, Portugal

Corresponding author: tiago.silva@i3bs.uminho.pt

ABSTRACT

Marine resources have been attracting the attention of scientists, engineers and clinicians as source of relevant compounds for the development of biomaterials with therapeutic potential, which need to have components mimicking tissue and to have the ability to better integrate with host tissue and promote its healing. The bioactive silica particles from different origins, i.e. silica from the deep-sea marine sponge *Geodia barretti* (GB), diatomaceous earth, and 45S5 Bioglass® particles, combined with alginate were used in the development of ink formulations. The 3D printed scaffolds biosilica:alginate (BS:Alg) with a triangular infill pattern architecture were fabricated, followed by coating with 0.5% and 1% collagen in 10 mM HCl (w/v) solutions. The fabricated scaffolds were characterized by the use of physicochemical, mechanical, and biological methods. Micro-CT results revealed good interconnectivity and porosity of the scaffolds, with the bioglass:alginate scaffold presenting the smallest mean pore size. Under bioactivity assessment of scaffolds without collagen coating via *in vitro* simulated body fluid (SBF) assay, calcium phosphate formation was observed at day 14 of incubation in SBF, demonstrating the potential of the scaffolds´ composition to support tissue mineralization. Biological evaluation of scaffolds revealed that the addition of collagen, in general, increased the cell adhesion in the scaffold. Additionally, on day 7 of culture, the BG:Alg scaffolds coated with 0.5% collagen demonstrated a significantly superior amount of DNA compared with the ones without collagen and with 1% collagen coating and, more relevant, to the ones produced with other silica-based materials.

Keywords: Marine sponge-derived biosilica, diatomaceous earth, bioglass, alginate, collagen, 3D printing, marine biomaterials, bone tissue engineering.

1. INTRODUCTION

Over the past few decades, researchers have proposed different strategies involving the development of new biomaterials for bone tissue regeneration (Chen, 2013; Lacerda, 2018; C. Wang et al., 2020). 3D printing is a technology with significant potential for engineering tissues that could mimic healthy native tissue (Atala, 2020; C. Wang et al., 2020). It has been known that anionic polysaccharide alginate is widely used as a scaffolding component for bone and cartilage tissue regeneration (Axpe & Oyen, 2016), as this biopolymer, extracted from brown algae (Benslima et al., 2021; Mohd Fauziee et al., 2021), is known to form hydrogels by ionic crosslinking using divalent cations as Ca^{2+}. Besides, a combination of silica and alginate hydrogel was used in the generation of new 3D composite biomaterials (Soni, Roopavath, Mahanta, Deshpande, & Rath, 2018) (Kong, et al., 2019). Besides being found in several minerals combined with different components, silica can be found in natural sources as deep-sea sponges and diatoms (biosilica) or synthesized in the laboratory (Jones, Brauer, Hupa, & Greenspan, 2016) (Hege & Schiller, 2015). Sponge-derived biosilica has the potential to be used in the fabrication of biomaterials for bone tissue regeneration (Dudik et al., 2018), as it possesses important properties, such as stimulation of mineralization and osteoblast-like cells proliferation (Xiaohong Wang, Schröder, Grebenjuk, et al., 2014). Nevertheless, it has not been yet applied as a bone substitutive material that can address clinical requirements for biomaterials (Zhang, Yang, Johnson, & Jia, 2019). The bioactive potential of biosilicas from marine sponges *Geodia barretti* (GB), *Geodia atlantica* (GA), *Stelletta normani* (SN), *Axinella infundibuliformis* (AI), and *Phakellia ventilabrum* (PV) for bone tissue engineering applications was evaluated by Dudik *et al.* (Dudik, O. 2021). The result of their study revealed the non-toxic behavior of biosilicas toward L929 and SaOs2 cells at a concentration up to 100 $mg \cdot mL^{-1}$, except for biosilica from GA sponge, that presents non-toxic effect at concentration up to 10 $mg \cdot mL^{-1}$. Moreover, researchers showed that GA-derived biosilica promotes the highest amount of calcium phosphates deposited on its surface during incubation in simulated body fluid up to 28 days. The biomedical potential of sponge-derived biosilicas is also supported by works by Gabbai-Armelin *et al.* and Barros *et al.*, demonstrating non-cytotoxic character of bioceramics from different sponge species (Gabbai-Armelin et al., 2019; Barros et al., 2014, 2016; Pallela & Ehrlich, 2016; Xiaohong Wang et al., 2012; Xiaohong Wang, Schröder, et al., 2014; Xiaohong Wang, Tolba, et al., 2014)

To fabricate 3D scaffolds, ink formulation should meet the required parameters for printing, such as well-controlled viscoelastic response (Bootsma, et al., 2017); that is, the biomaterial ink must be able to flow through a deposition nozzle and then “set” immediately

to facilitate shape retention of the deposited features even as they span gaps in the underlying layers (Guvendiren, Molde, Soares, & Kohn, 2016). The rheological properties must be evaluated to optimize the printing capacity and biomaterial ink stability, aiming to achieve the best possible printing fidelity is respect to the established 3D design (Murata, 2012). This design should render adequate porosity and interconnectivity enabling cell migration and proliferation towards the population of the entire scaffold (Karageorgiou & Kaplan, 2005) (Stevanovic, et al., 2013) (Bose, Vahabzadeh, & Bandyopadhyay, 2013), while resulting in mechanical properties matching the ones of the target tissue (Anderson, 2016) (Jakus, Rutz, & Shah, 2016). For biomaterial ink production, alginate hydrogel could be a good candidate for mimicking large glycosaminoglycan hyaluronic acid of extracellular matrix (ECM) due to its biocompatibility, non-toxicity, elasticity, ability to absorb water in large quantities and control the mineral formation (Sargus-Patino, 2013) (Hunt, Shelton, & Grover, 2009) (Tan, et al., 2014). The collagen used in biomaterial fabrication could simulate the properties of natural ECM collagen, providing biochemical cues for cell adhesion (Akhir & Teoh, 2020; Sousa et al., 2020).

Therefore, the present study describes the development of biomaterial ink formulations based on silica from different sources, i.e. bioactive glass (BG), biosilica from GB sponge and DE biosilica particles, and alginate for 3D printing. GB:alginate, BG:alginate and DE:alginate 3D scaffolds were developed followed by collagen coating. Afterward, obtained biomaterials were characterized regarding morphological and mechanical features. Bioactivity and cytocompatibility of 3D-printed biosilica:alginate scaffolds were evaluated in comparison with BG:alginate and DE:alginate scaffolds envisaging application for bone tissue engineering.

2. MATERIALS AND METHODS

2.1. Materials

Geodia barretti (GB) sponge samples were collected in Korsfjord, Norway and kindly provided by Prof. Hans Tore Rapp and Dr. Joana Xavier from University of Bergen. Diatomaceous earth (DE), named Diatomit – Fossil Shell Flour® (89 - 92 % SiO_2) used in the present work, was provided by Perma-Guard Europe Sollaris (Poland), and have been obtained from *Melosira preicelanica* fossils from freshwater. A bioactive glass, 45S5 Bioglass® (BG) with the following composition: 45% SiO_2, 24.5% Na_2O, 24.5% CaO, and 6% P_2O_5 (wt. %), was supplied by NovaMin Technology (Alachua, Florida, USA). Sodium Alginate (PanReac AppliChem, Spain), from *Macrocystis pyrifera* brown algae, sodium hydroxide (PanReac AppliChem, Spain), acetic acid (Honeywell Research chemicals, USA) and hydrochloric acid (Honeywell Research chemicals, USA) were used as received.

2.2. Isolation of biosilica from the marine sponge

To obtain biosilica particles from deep-sea sponge GB, the sponge chunks were washed with ultrapure water to remove ethanol solution in which were preserved and sea residues, and then calcinated at 600 °C for 6 hours, using a heating ramp of 10 $ºC \cdot min^{-1}$ followed by a dwelling time of 6h at that temperature, and cooling down to room temperature. The extracted biosilica powder was milled using an Ultra-Centrifugal Mill ZM 200 (Retsch, Germany) and sieved in Sieve Shaker (Retsch, Germany) to obtain silt from the particles, with size in the range of > 36 μm and < 63 μm. The DE and BG were size standardized with the same size before use as well.

2.3. Collagen production

Collagen extraction was performed using *Gadus morhua* codfish skins (Mar Lusitano, Gafanha da Nazaré, Portugal) generated as by-products from codfish processing. Skins were cleaned and washed with distilled water to remove any residual debris. Then, skins were treated with 0.1M NaOH (1/10 w/v) solution under stirring for 72h. The basic solution was replaced every 24h for the removal of impurities and non-collagenous proteins. After that, the skins were washed with distilled water until obtaining the neutral pH and further immersed in 0.5 M acetic acid solution (1:10 w/v) for the next 72h. After centrifugation, the supernatant was salted out with the 0.9M NaCl, followed by centrifugation at 20,000 g for 30 min. The obtained collagen dissolved in 0.5M acetic acid (1:1 v/v) was purified by dialysis against 0.1M acetic acid solution for 48h, followed by dialysis against 0.02M acetic acid solution for 48h, and distilled water until reaching the neutral pH according

to the protocol described in the work by Sousa et al. (2020). The purified codfish collagen type 1 (COL1) was dissolved in 10 mM HCl to prepare 1% and 0.5% w/v solutions of COL1.

2.4. Physicochemical characterization of biosilica particles

2.4.1. Fourier-transform infrared spectroscopy

The structural characterization of biosilica particles was performed using Fourier-transform infrared spectroscopy (FTIR) with attenuated total reflectance mode (FT-IR ATR) on IR Prestige-21 (Shimadzu, Japan) in a wavenumber region of 4000-400 cm^{-1} at room temperature.-The spectra were collected as an average of 32 scans with a resolution of 4 cm^{-1}. Potassium bromide was used to dilute the sample powders.

2.4.2. X-ray diffraction

The crystalline character of the silica powders was evaluated by X-ray diffraction (XRD) measurements performed using a conventional Bragg-Bretano diffractometer (Bruker D8 Advance, Germany) equipped with CuKα radiation. X-ray diffraction data were collected from 5° to 50° on a 2θ range in the step of 0.04° and 1 s for each step.

2.4.3. Scanning electron microscopy - Dispersive X-ray spectroscopy

The morphology of all silica powders was examined by Scanning electron microscopy (SEM) using a JSM-6010 LV microscope (JEOL, Japan) equipped with an energy-dispersive X-ray spectroscope (EDS) (Oxford Instruments, United Kingdom). The working distance of 10–12 mm and beam energy of 10.0 kV were applied. Before SEM analysis, biosilica samples were platinum-coated. EDS analysis was performed at three different points using beam energy of 15.0 kV and magnification of 35X, 200X, and 1000X. The EDS spectra were presented after analyses using the Aztec software (Oxford Instruments, UK).

2.4.4. Thermogravimetric analysis

Thermogravimetric analysis of the biosilica samples was carried out on Simultaneous Thermogravimetric Analyzer STA7000 (Hitachi, Japan) under nitrogen and oxygen atmosphere at a flow rate of 150 and 50 $mL \cdot m^{-1}$, respectively. 4.5 - 5 mg of sample was placed in the platinum sample holder and analysis was performed in a temperature region from 23 to 600 °C using a heating rate of 10 $°C \cdot min^{-1}$.

2.5. Ink formulation preparation and its characterization

To select the appropriate concentration of alginate needed to prepare biosilica-based inks, the aqueous solutions of sodium alginate at 8 % (wt. %) were prepared and analyzed. The viscosity of the prepared solution was measured using a rheometer (Kinexus

pro+, Malvern, UK) over a shear rate range of 0.01–100 s^{-1} with a cone (4° angle and 40 mm diameter) and plate geometry. After the alginate test, the inks formulations used for printing were prepared using a ratio of 100 mg of silica-based material (GB, DE, or BG) to 1 mL of alginate 8% (wt. %) solution. The silica powders were dispersed in alginate solution with dispersion device Ultra-Turrax® (IKA Werke, Germany) followed by crosslinking with 50 µL of 7.5 % (wt. %) $CaCl_2$. This is an important step since $CaCl_2$ crosslinks the polymeric alginate chains, increasing the solution viscosity, thus allowing better control of the extrusion process. The apparent viscosity of the inks was measured in viscometry mode using the same rheometer and with the same condition used for the characterization of alginate solutions. The viscoelastic properties were assessed using a plate with a radius of 20 mm and a gap of 1 mm in the oscillatory mode. Frequency sweep experiments were performed with 1% of shear strain (within in a linear viscoelastic region (LVR), previously determined), over a frequency range of 0.01–100 Hz (Walls et al., 2003). All dynamic experiments were performed at 25 °C and in triplicates.

2.6. 3D printing of biosilica-based scaffolds

The 3D printing process was performed using a customized extrusion-based 3D Printer (Regemat 3D, Spain). The scaffolds were designed via internal equipment software with 10 layers at the height of 3 mm and a triangular infill pattern, resulting in a 15 mm^2 structure with 500 µm pore size. The dispensing nozzle of 0.41 mm diameter was attached to the syringe. The printing was executed at room temperature (RT), with a stationary table and spindle X, Y, and Z axes, at a flow rate of 2 $mm \cdot s^{-1}$ and a printing speed of 10 $mm \cdot min^{-1}$. The equipment resolution of X and Y is 150 microns and of Z is 400 microns. After printing, the scaffolds were immersed in 7.5% (wt.%) $CaCl_2$ solution for 24 h at RT (as the second cross-linking step). The crosslinked scaffolds were cut into smaller cylindrical samples of 4mm and 6mm in diameter, which were subsequently washed with ultrapure water to remove the salt solution, frozen at − 80 °C, and subsequently freeze-dried. Scaffolds for *in vitro* biological tests were sterilized with ethylene oxide at 45 ºC for 4 h.

2.7. Collagen coating process

After the sterilization process, the scaffolds were divided into three groups: scaffolds without coating, scaffolds with 0.5% COL1 and 1% COL1 coating. To coat the scaffolds with marine collagen, the solutions of COL1 0.5% and 1% in 10 mM HCl (w/v) were dropped on the top of the scaffolds, namely 20 µL and 40 µL of each solution were used for coating of the scaffold with 4 mm- and 6 mm-diameter, respectively, followed by crosslinking with the same corresponding volumes of 60 mM 1-ethyl-3-(3-dimethylaminopropyl) carbodiimide

hydrochloride (EDC). After an overnight crosslinking reaction, the scaffolds were washed twice with ultrapure water, frozen at − 80 °C, and freeze-dried.

2.8. Scaffolds' characterization

The scaffolds were characterized according to the proposed design and composition. The morphological, physicochemical, thermal and mechanical characteristics of the developed scaffolds were evaluated with a series of methods described below.

2.8.1. Morphological analysis

The morphology of developed scaffolds (filament width, layer height, pore size, porosity, and interconnectivity) was assessed by micro-computed tomography (micro-CT) and SEM. Scaffolds' microarchitecture was evaluated through an X-ray diffraction technique using a high-resolution micro-CT SkyScan 1272 (Bruker, USA). For image acquisition, the selected parameters were as follows: a pixel size of 6 μm, a voltage range of 35 kV, and a current source of 180 μA (version 1.1.3). All samples were acquired over a rotation angle of 360°, with a rotation step of 0.45°. Data sets were reconstructed using a standardized cone-beam reconstruction software (NRecon version 1.6.10.2), and representative slices were segmented into binary images with a dynamic threshold between 25 – 255. After that, the binary images were used for morphometric analysis (CT Analyzer, v1.15.4.0, Bruker) and to build the 3D models (CTvox, version 3.0.0). Quantitative information of total porosity (%), pore size (μm), and interconnectivity (%) were assessed. The results are the mean of three measurements per formulation.

The theoretical porosity of the scaffolds was calculated using the equation.

$$Porosity = 1 - \frac{V\ solid}{V\ total} * 100(\%)$$

Where $V\ solid$ is the volume of the scaffold, and $V\ total$ is the volume determined by the dimension of the scaffold (LxWxT).

The morphology of the scaffolds, pore size, filament width, and layer height were determined using SEM. The samples were coated with a thin layer of platinum (approx. 2 nm) before the analysis. The analysis was carried out with beam energy of 10 kV and at 35X, 150X, 300X, and 1000X magnification.

EDS was used to analyze the surface elemental composition of scaffolds at 40X and 200X magnification.

2.8.2. Mechanical tests

The mechanical characterization of silica:alginate (S:Alg) scaffolds was performed using uniaxial compression tests according to ASTM F2064 – 17 on a universal testing machine (model 5543, Instron, UK) using a load cell of 50 N and a crosshead speed of 1 $mm \cdot min^{-1}$, until the maximum load of the scaffold's architectures or equipment load cell limit. The compressive stress and strain were recorded for every 20 ms, and the compressive modulus was calculated by the slope of the stress-strain linear region before failure (in the range of 10-15%). At least 5 specimens were tested for each composition.

2.8.3. Thermogravimetric analysis

Thermogravimetric analysis (TGA) of the printed scaffolds was performed on a Simultaneous Thermogravimetric Analyzer STA7200 (Hitachi, Japan). Samples (2-4 mg) were placed in a platinum crucible and an empty crucible was used as reference. The samples were heated from 40 ºC to 600 ºC at 10 $ºC \cdot min^{-1}$ and held at that temperature for 20 min, under an air simulating atmosphere (nitrogen (79%)/oxygen(21%)) with a flow rate of 200 $mL \cdot min^{-1}$. The mass change was recorded as a function of temperature. Each sample was measured in triplicate.

2.9. *In vitro* bioactivity via assay in simulated body fluid (SBF)

To evaluate the apatite formation on the material surface, the bioactivity test was performed by incubating 3D printed scaffolds without COL1 coating in SBF for up to 21 days, under different time points of analysis (1, 3, 7, 14, and 21 days). The assay was conducted according to ISO 23317:2014. The test was done in triplicate. SBF was prepared with an ion composition that is similar to that of human blood plasma following the protocol described in work by Kokubo *et al.* (Kokubo, Kushitani, Sakka, Kitsugi, & Yamamuro, 1990). Each scaffold was inserted into a plastic tube containing 15 ml of SBF. Afterward, the tubes were placed in a water bath at 37 °C under shaking. At each time point, the scaffolds were removed from SBF and washed thoroughly with ultrapure water. SEM/EDS was used to analyze the surface of scaffolds previously dried at 37 °C.

2.10. Cell culture assays using SaOS-2 cell line

2.10.1. Culture, expansion and seeding of osteosarcoma (SaOS-2) cells

The cell culture assay was performed to evaluate cell attachment and cytocompatibility (Tamburaci & Tihminlioglu, 2018) in the scaffolds of GB:Alg, DE:Alg, and BG:Alg scaffolds, with 0.5%, 1%, or without COL1. The SaOS-2 cell line was chosen in this

study as model of osteoblasts. The cells were unfrozen from -80 ºC and incubated in a T75 flask with Dulbecco's Modified Eagle's medium-high glucose (DMEM) (Merck, Germany) supplemented with 10% v/v of fetal bovine serum (FBS) (Thermo Fisher, USA) and 1% v/v of penicillin-streptomycin (Thermo Fisher, USA). The culture medium was refreshed every 2–3 days. SaOS-2 cells were harvested at pre-confluence using the TrypLE™ solution. Cells were used between 7 and 9 passages. The cells were seeded using top-down approach in a 48 well-plate for suspension culture by dropping 20 µL with a cell density of 150.000 cells/scaffold followed by scaffolds incubation for 1h to allow cell attachment. After that, 300 µL of culture media as previously described were added to each well. The culture medium was changed after every 3 days. Three different culture time points were evaluated, namely 1, 3, and 7 days.

2.10.2. Cytotoxicity assay

The cytotoxicity studies were carried out at predefined culturing time points. The relative cell viability was evaluated by Alamar Blue Assay using the Alamar Blue® kit (Bio-Rad, USA), following the manufacturer's instructions (Bio-Rad). Briefly, after the addition of Alamar Blue reagent 10% v/v, the scaffolds were incubated at 37 °C with 5% CO_2 for 3h. Then the fluorescence intensity was read at 530/590 (excitation/emission) using a microplate reader (Synergy HT, Bio-Tek, USA).

2.10.3. DNA quantification

Cell proliferation assays were carried out at the same culturing period as for cytotoxicity assay. Briefly, the scaffolds were collected and washed with Tris-Buffered Saline (TBS) (Thermo Fisher Scientific, USA), and then transferred to 1.5 mL microtubes containing 1 mL of ultrapure water. After incubation at 37 °C for 1h, the microtubes with scaffolds were frozen at -80 °C until use. To lyse the cells, the scaffolds were thawed and placed in an ultrasound bath for 30 min. The DNA analysis was done using a Quant-iT™ PicoGreen® Kit, (Thermo Fisher Scientific, USA), according to the manufacturer's instructions. The DNA concentration was calculated from a calibration curve generated using DNA standards at a concentration range of 0 – 2 $\mu g \cdot mL^{-1}$. The fluorescence intensity was read at 485/528 (excitation/emission) on a microplate reader (Synergy HT, Bio-Tek, USA).

2.11. Statistical Analysis

The data are represented as mean ± standard deviation SD. The Shapiro–Wilk test ($p < 0.05$) was used to check the normality of the data distribution ($p < 0.05$). For non-parametric values, the data were analyzed using the Mann-Whitney test. For parametric values, a t-

test was used. Significant differences are marked with **** for $p < 0.0001$, *** for $p < 0.001$, ** for $p < 0.01$, and * for $p < 0.05$.

3. RESULTS AND DISCUSSION

In this study, we evaluated the potential of the biosilica from *Geodia barretti* in comparison with other silica-based material to be used for bone tissue engineering applications. We introduce the reader to physicochemical and morphological properties of the particles, the process of the biomaterial formulation ink production and 3D printing, the characterization of scaffolds' properties by physicochemical, biological and mechanical assays.

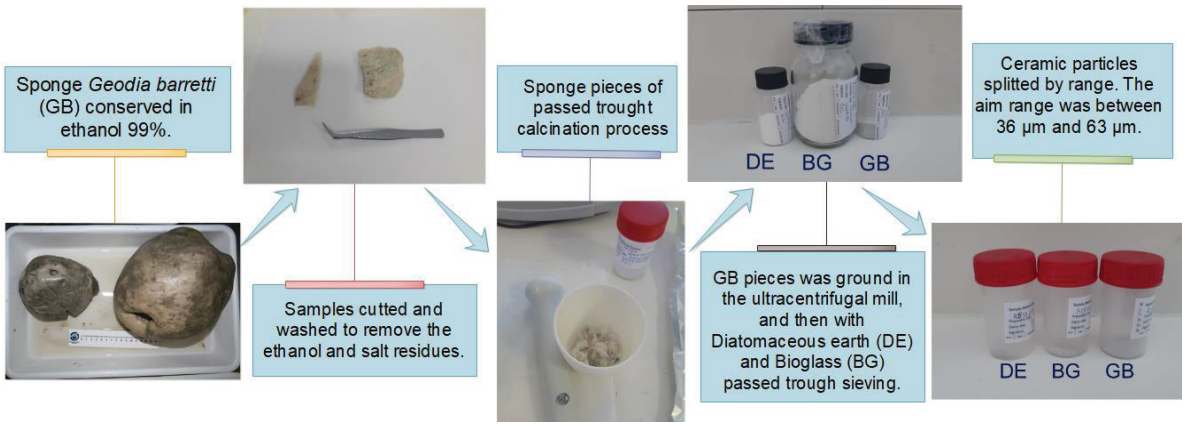

Figure 2. Particles' standardization scheme.

3.1. Physicochemical analysis of biosilica particles

The biosilica bioseparation from the GB sponge included the calcination process at 600 ºC to remove the organic portion. This calcination temperature was chosen as a consequence of the results based on TG analysis of GB sponge in the work by Dudik O. *et al*. (Dudik et al., 2021). The authors demonstrated that the organic part of the marine sponge undergoes thermal decomposition in the temperature range 200 - 544 ºC and final removal when temperature increases. In comparison to previous work and the described calcination, at 600º C it is already possible to obtain biosilica with differentiation in crystal-forming at 16.6º and the physical properties of this could be investigated.

The calcination process efficacy was confirmed by elemental characterization of the sample before and after the calcination process using the EDS method (Table I). The absence of carbon in GB after calcination confirms a complete removal of the organic portion from the sponge. From Table I GB and DE particles are mostly composed of SiO_2. EDS analysis showed 2.9 wt% of Al in the structure of DE and minor concentrations of additional ions, i.e. S, Na, Ca, P, K, Mg, and Al, in GB-derived structure. The elemental analysis of GB-derived biosilica obtained in the study of Dudik et al. (Dudik et al., 2021) as well revealed the traces of the listed ions, among which the Al content was 6.5 times higher

(1.3 wt%). EDS analysis of BG showed the presence of O, Si, Na, Ca and P in its structure proving its chemical composition.

Table I. Elemental composition of silica particles.

Element (Wt%)	C	O	Si	S	Na	Ca	Cl	P	K	Mg	Al
BG	0	50.5	16.1	0	13.7	17.6	0	2.1	0	0	0
DE	0	53.8	43.3	0	0	0	0	0	0	0	2.9
GB raw material	56.9	32.5	8.4	0.6	0.3	0.3	0.3	0.2	0.2	0.2	0.1
GB after calcination	0[a]	57.8	37.9	0.2	1.5	1	0	0.6	0.4	0.4	0.2

[a] The process of calcination was successful due to the absence of carbon in the structure of GB-derived silica.

The crystallography analysis by XRD revealed that particles of BG and DE present amorphous structures as shown in Figure 3-A. In contrast to them, the crystallography analysis demonstrated a crystallization of GB-derived biosilica after the sponge calcination process, which can be a good sign for a biomaterial in terms of physical stability (Murali, Ramamurty, & Shenoy, 2008). The XRD spectrum of GB-derived biosilica presents an intense peak at 16.6º and small peaks at the range from 18° to 35° which could be related to zeolite formation during the calcination process, time and temperature, and the processed by-products by the marine sponge (Liu, et al., 2019). In the work by Dudik *et al.* (Dudik et al., 2021) the XRD pattern of GB-derived silica presented a strong peak around 22°, revealing the transition of silica from amorphous to cristobalite. It was explained by the fact that cristobalite formation occurred during the extraction process of silica upon sponge calcination at 800 °C. In the present study, the temperature used for sponge calcination was 600 °C. In our study, the less intense XRD peaks in the range from 27° to 32° for the GB sample could be assigned to cristobalite (Shuang-Hong Xue, Hao Xie1, Hang Ping, Qi-Chang Li, 2018).

The structural bonds and functional groups of silicates were found in the silica particles as presented in Figure 3-B. There are peaks in IR spectra of GB-based biosilica and DE that can be attributed to the asymmetrical and symmetrical stretching vibrations of Si-O of the SI-O-Si network, namely at 1100 cm^{-1} (DE), at 1050 cm^{-1} (GB) and 797 cm^{-1} (DE and GB). The peak observed in the spectrum of BG at 960 cm^{-1} is related to vibrations of the silanol group, and the broad peak around 3450cm^{-1} is related to stretching vibrations of

the O-H bond in the silanol group (Karbowiak, et al., 2010). The band at 1646 cm^{-1} corresponds to adsorbed water.

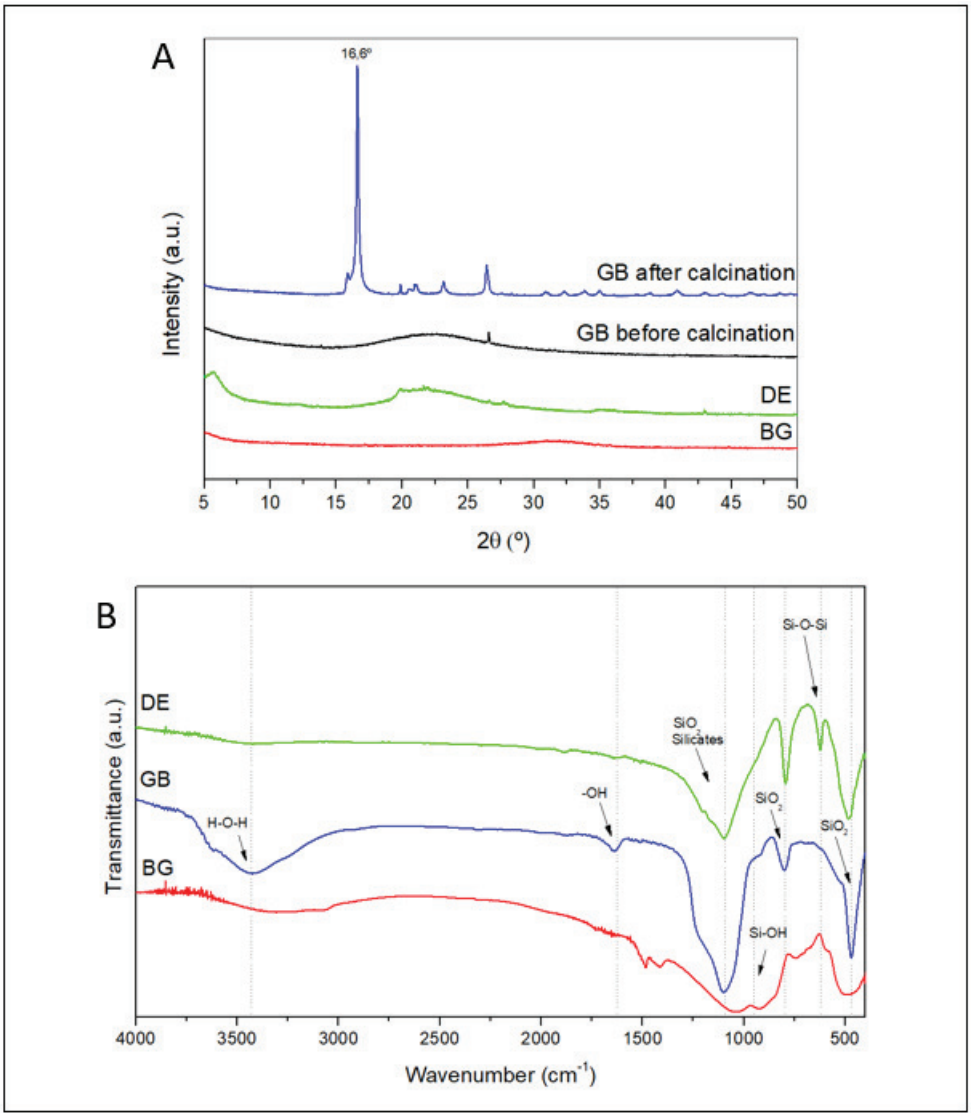

Figure 3. Graphical identification of biosilica particles: **A** and **B** figures are the FTIR spectra and XRD diffractograms respectively for the different biosilica (DE, GB, and BG).

The morphological features of biosilica particles are displayed in SEM micrographs in Figure 4. The particles of all biosilicas presented different sizes and shapes. It is also evident that morphological features of biosilica particles strongly depend on the silica source. The DE presented the fossil shells as cylindrical structures with a hollow interior and nanopore walls, the BG presented structures in irregular shapes with approximate three-dimensional dimensions, like broken cubes and sizes within the defined pattern. Finally, the GB particles represented sponge spike structures (siliceous spicules), with a greater presence of sterrasters (spherical) and dichotriaenes (rod-like) that were broken

during the calcination process and grinding. To standardize the particles by size, the sieving was performed with sieve pore sizes between 36 to 63 µm. The particle's standardization makes it possible to obtain a specific range, important to avoid clogging the syringe. However, some GB-derived biosilica particles with a size larger than 63 µm passed through the sieve, as shown in Figure 4.

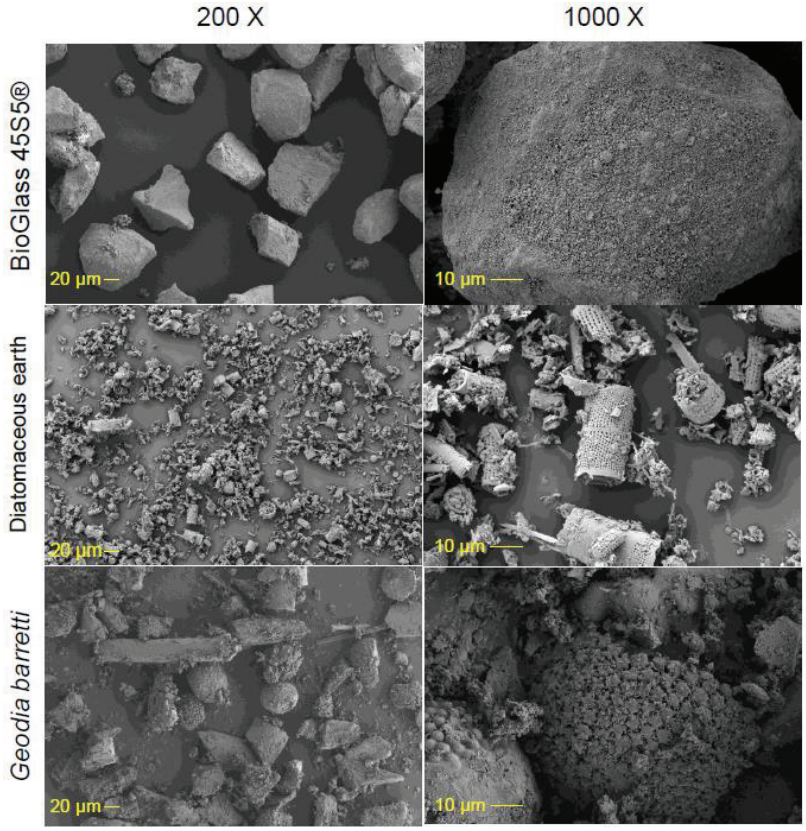

Figure 4. SEM micrographs of the silica-based particles particles at 200X and 1000X magnification.

3.2. Rheological characterization of biomaterial ink formulations

The fabrication of 3D printed BS:Alg scaffolds comprised several steps, such as optimizing the Alg hydrogel concentration and the ratio between BS particles and polysaccharide solution for preparation ink formulation and printing parameters setup. Furthermore, one of the essential printing parameters is correlated to the rheological characteristic of the Alg hydrogel and biomaterial ink formulation. For instance, the material viscosity impacts the printing accuracy. Figure 5-A represents the rheological behavior of ink formulations, showing that the addition of BS to 8% alginate solution at a concentration of 1:1 (w/v) resulted in higher viscosity values at shear rates up to 10^2 s^{-1}. However, there is no significant difference in viscosity between ink formulations with different BS particles.

Oscillatory tests results are depicted in Figure 5-B showing viscoelastic properties of biomaterial ink formulations and Alg hydrogel as control. The viscoelastic modulus presented a stable behavior in different frequencies, with small differences between BS particles.

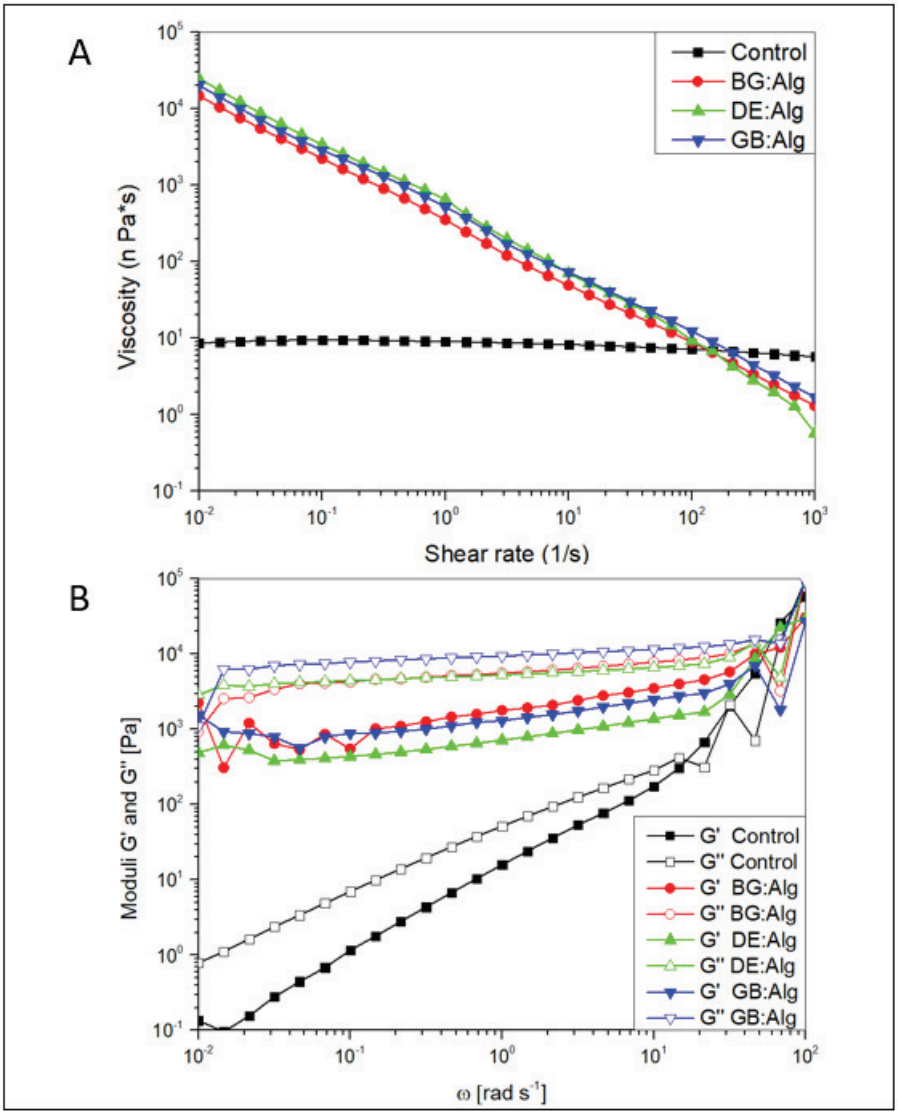

Figure 5. Rheological studies BS:Alg inks and control (Alg 8% wt.) **A** - Viscosity versus shear rate and **B** - G' - storage modulus and G'' – loss modulus versus frequency.

The concentration of alginate hydrogel makes possible the good dispersion of these BS particles with the assistance of Ultra-Turrax® and followed by the crosslinking with $CaCl_2$ 7.5%. It is important to observe that this biomaterial ink should be performed at the same time as printing, to avoid the BS weight could affect the dispersion. Other study related the how the addition of bioactive glasses in polymers - for biomaterial inks production - could decreases the sol-gel transition temperature, and particle size as well can affect (Zeimaran

et al., 2021), in comparison to this data, the size standardization of our BS particles seems to assure the stability of the biomaterial inks G' and G'' moduli.

3.3. Morphological analysis of produced scaffolds

Scaffold porosity and interconnectivity are essential attributes in biological performance since they influence the mechanical properties of the constructs and can play a significant role in cell adhesion, proliferation, and vascularization. It has been shown that ideal scaffolds for bone tissue engineering strategies should have a 3D architecture with 150-500 μm pore size to enable cell migration into the scaffold core towards complete population of the structure (Dai, et al., 2015) (Roohani-Esfahani, et al., 2013). In our study, the design of the scaffold porous structure comprised a 500 μm pore size a 410 μm dispensing nozzle (influencing the diameter of the printer struts). From the microscopic observation of scaffolds (Figure 6), it can be observed that the freeze-drying process affected their structure by the reduction of pore size and appearance of fractures. Micro-CT analysis also confirmed the decrease of pore size in scaffolds´ structure (Figure 7). The DE-based scaffolds (0 % COL1) presented a smoother surface compared with other scaffolds, as it showed on SEM micrograph in Figure 6. To improve cell attachment to 3D printed constructs, the BS:Alg scaffolds were coated with COL1. From SEM images of scaffolds with 0.5 and 1 % of COL1, we can notice COL1 nets formed between pores and on the surface of 3D scaffolds.

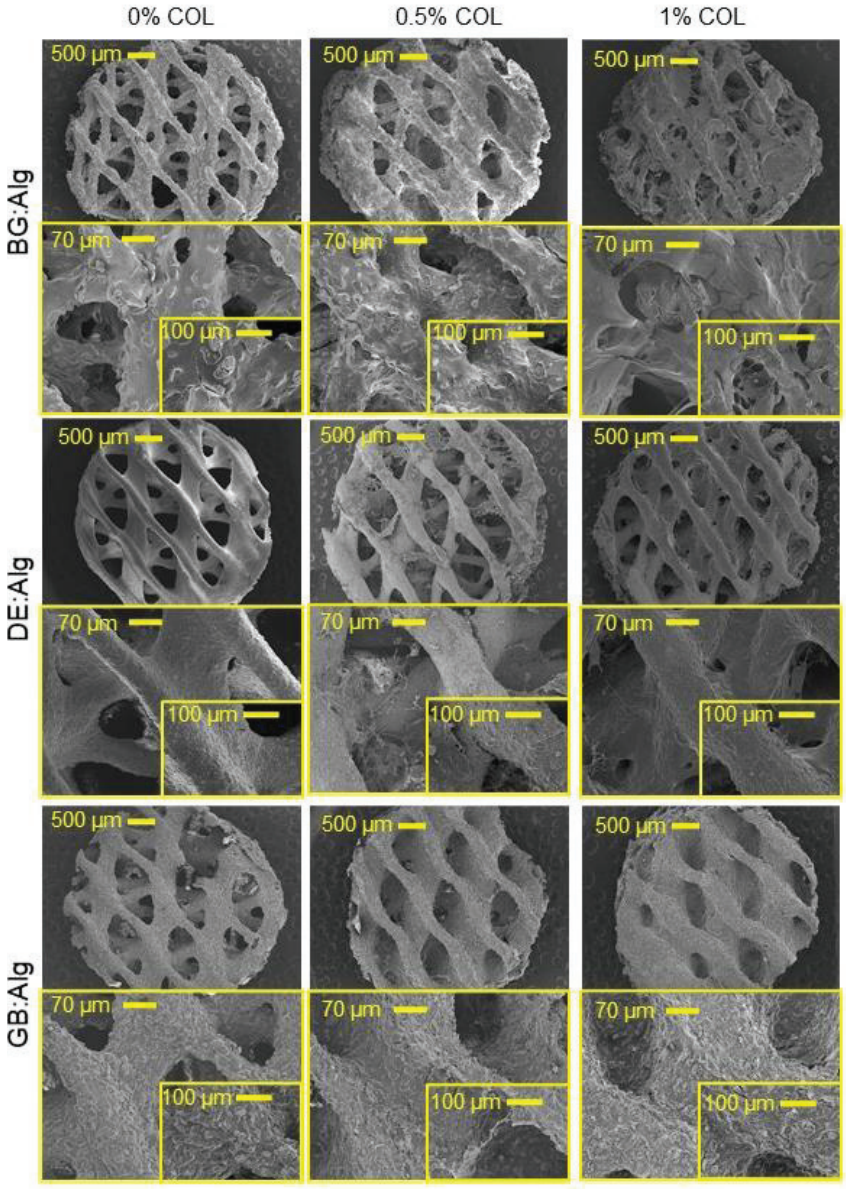

Figure 6. SEM images of BS:Alg scaffolds with and without COL1 coating with 20X, 70X and 200X magnification.

The Micro-CT analysis is a technique with various key advantages for architecture evaluation and morphological assessments since it is non-destructive, samples remain intact for further assays (Ho & Hutmacher, 2006). In our study, Micro-CT was performed to evaluate the pore size, porosity, and interconnectivity, and a representative image of the samples is presented in Figure 7-A. It was found high interconnectivity (>90%) for all scaffolds, except GB:Alg + 1% COL1 (Figure 7-B), which presented 87.98%. Moreover, the mean pore size of the 3D printed scaffold (Figure 7-C) is inversely proportional to the COL1 concentration, for DE:Alg and GB:Alg. For BG:Alg scaffolds with or without coating presented lower pore values, in comparison with other 3D printed scaffolds. The BG

particles' weight, shape, density and distribution could affect the BG:Alg scaffolds, (Figure 5), into aggregation or even coalescence effect, which in turn leads to less aggregation in biopolymer during obtaining ink formulation and increasing pore size during 3D printing process. The total porosity (Figure 7-D) of BG:Alg scaffolds increases proportionally to the COL1 coating concentration, presenting a higher value in comparison to the others. DE:Alg scaffolds present a lower percentage of total porosity. It could be explained by the particles of DE are formed by micro aggregates, and when dispersed during the 3D printing process, could have higher aggregation within the COL1 matrix, and that results in the formation of the larger pores in DE:Alg scaffolds without COL1 coating.

From the Micro-CT analysis of pore size, the COL1 coating caused a decrease in pore size in DE:Alg and GB:Alg scaffolds, as expected, by the increment of the COL1 coating material within the scaffold pores size. This pore reduction could be observed, as another study for bone scaffolds (Peyrin, 2011) and for diatom as biosilica and chitosan polymer (Tamburaci & Tihminlioglu, 2018), both performing Micro-CT, observing different materials-base scaffolds and the pore size impact for the bone regeneration, since they observed the neovascularization after implants, in comparison to biological *in vivo* experiments and other techniques, as histology.

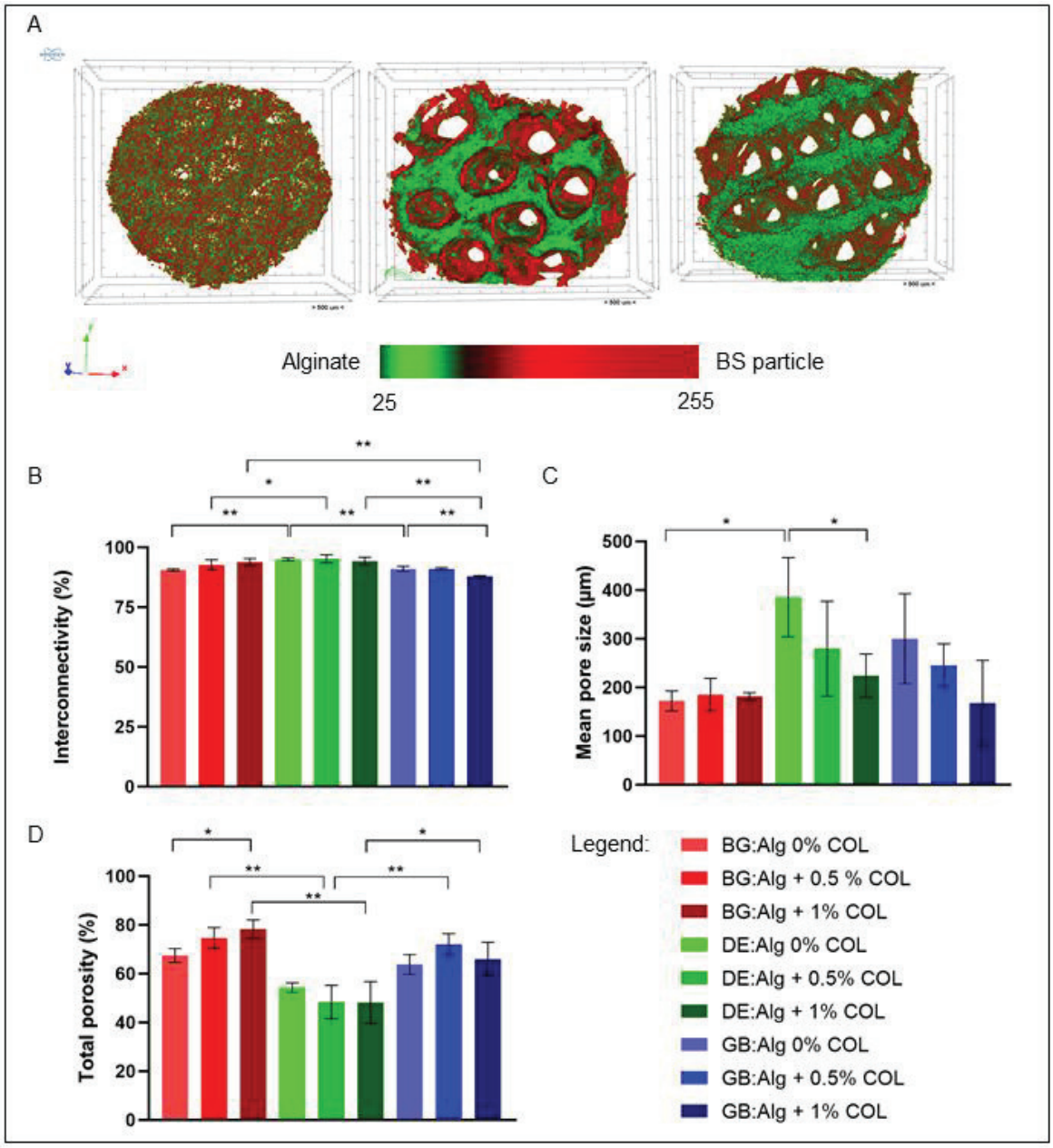

Figure 7. Micro-CT structural analysis of 3D printed BS:Alg scaffolds with and without COL1 coating **A** – Representative image of samples. **B** - Interconnectivity of all BS:Alg scaffolds seem above 80%. **B** - BG:Alg presents higher total porosity in comparison to other BS:Alg scaffolds, and **C** - The mean pore size of BS:Alg scaffolds present a reduction with a collagen coating, except for BG:Alg scaffolds. Data in the graphics are presented as mean ± SD and the statistical differences are presented with * for $p < 0.05$ and ** for $p < 0.01$.

3.4. Mechanical properties

BS particles from a different origin, even with standardized size, have particularities in morphological structure, that could influence on mechanical properties of fabricated materials. The compression assay was performed to evaluate the mechanical properties of BS:Alg scaffolds without collagen coating and the determined compressive modulus values

are displayed in Figure 8-A. For the development of biomaterial mimicking cancellous bone tissue, the compressive modulus value of the engineered construct should be in the range of 0.12 – 1.1 GPa (or 120 – 1100 MPa) (Xiaojian Wang et al., 2016)(Vogl et al., 2017)(Keaveny et al., 2001). In our study, the mechanical properties of BS:Alg scaffolds presented a mean of 11.85 MPa and did not achieve the range proposed for cancellous bone or hard tissues and may be improved, or directed for non-load-bearing applications. DE:Alg scaffolds exhibited the highest compressive modulus, with a mean of 29.4 MPa, and GB:Alg the mean of 21.0 MPa. The addition of collagen coating onto 3D scaffolds may have a small influence on the compression resistance of the scaffold, but this was estimated as non-relevant and thus it was not determined.

3.5. Thermogravimetric assay

TGA of the developed scaffolds without COL1 coating was performed to evaluate the percentage of dry mass, corresponding to biosilica content. The total mass loss for BG-, DE- and GB-based scaffolds were 63.32%, 57.23% and 66.13%, respectively (corresponds to organic content) (Figure 8-B) and thus the inorganic content of the scaffolds was estimated as 36.68 %, 42.77%, 33.87% for BG, DE and GB, correspondingly. In our study, 100 mg of BS was dispersed in 1 mL (0.08 g mL^{-1}) of Alg upon preparation of ink formulation. TGA results revealed that the fabricated scaffolds have different mass ratios between organic and inorganic parts which may be caused by the difference in particle size that affected their distribution in the polymer matrix during the 3D printing process.

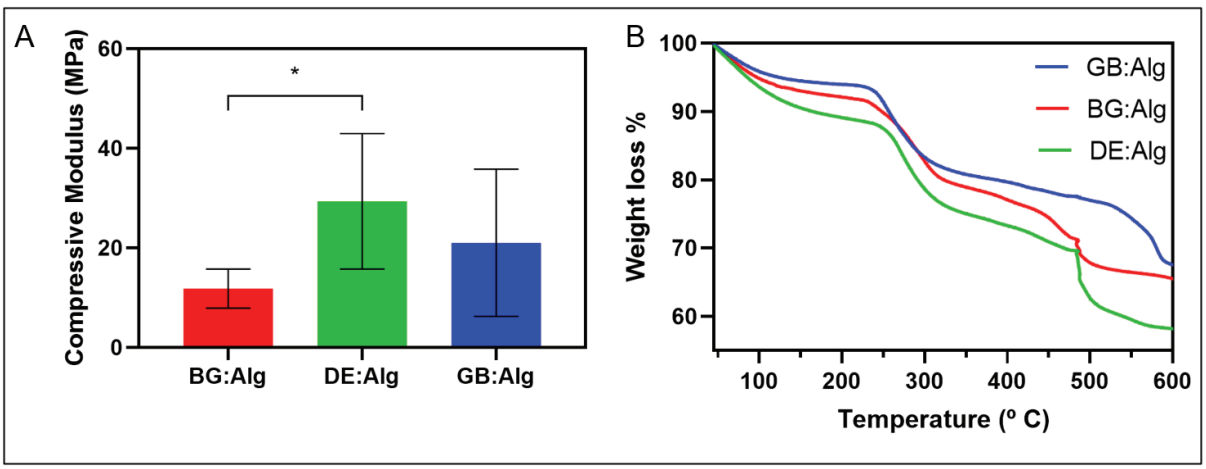

Figure 8. Structural assessments of BS:Alg scaffolds: **A** - The compressive modulus of BS:Alg scaffolds, and **B** - TGA curves of BS:Alg scaffolds presenting weight loss percentage as a function of the temperature. Data in the graphics are presented as mean ± SD and the statistical differences are presented with * for $p < 0.05$.

3.6. Assessment of scaffolds´ bioactivity via *in vitro* SBF assay

The surface of scaffolds after immersion in SBF at different time points was examined by SEM and EDS analysis. From Table II, which presents the evolution of elements' concentration of each BS:Alg scaffolds during the bioactivity via *in vitro* SBF assay, it can be noted that the concentration of P (from the phosphates) increases on the BG:Alg surface along incubation period time. An increase of Ca ions on BG:Alg scaffold was observed from day 1 to day 3, and the subsequent decrease from day 7 to day 14 showed release of ions to SBF. The maximum concentration of Ca ions on BG:Alg was achieved on day 21 days of incubation in SBF. In the case of DE:Alg the maximum concentration of Ca ions was observed on day 14. In contrast, for GB:Alg scaffolds, on day 1 the Ca concentration was almost halved and insignificantly changed up to 21 days of incubation in SBF. This behavior can be explained by the diffusion of ions from scaffolds to SBF and can be supported by the results from the study by Dudik et al. (Dudik et al., 2021) demonstrating a decrease of Ca ions on GB-derived biosilica surface during immersion time in SBF. Figure 9 demonstrates the formation of CaP deposits on the surface of 3D scaffolds after 14 days of incubation in SBF, followed by Table II, which presents the evolution of elements' concentration of each BS:Alg scaffolds during the bioactivity via *in vitro* SBF assay.

It was possible to evaluate the chemical composition and calcium phosphates deposition when immerse in Simulated Body Fluid using EDS, however, spectrometry could be used for further analysis. A study with alginate and BG scaffolds also observe an increment of Ca^{2+}, the differentiation was the SaOS-2 already encapsulated into biomaterial ink (Xiaohong Wang, Tolba, et al., 2014). A recent study using bioactive glass-alginate composition observed the these materials did not show any adverse effect on cell viability (Özarslan et al., 2021).Another study with biosilica from diatomaceous earth has noted the increment of this biosilica particle in the referred scaffold increased the Ca/P ratio in 7 and 21 day incubation (Tamburaci & Tihminlioglu, 2018).

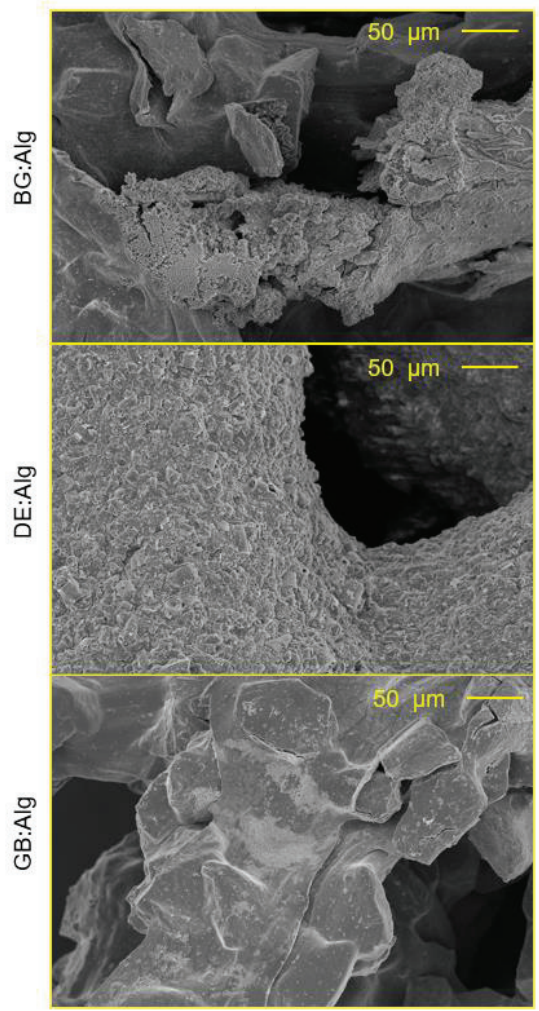

Figure 9. BS:Alg scaffolds after 14 days of incubation in SBF, SEM images at 300x magnification.

Table II. Scaffolds' bioactivity studies via in vitro SBF assay, tables of the elemental composition of scaffolds´ surface before and after incubation in SBF at different time points.

		Element concentration on weight %							
BG:Alg	Time (days)	O	C	Si	Na	Cl	P	Ca	Al
	0	48.1	34,0	1,3	1.0	4,5	0.2	10.9	-
	1	48,7	33,8	1,3	2,9	1,7	1,9	9,6	-
	3	48	25,2	0,4	3,7	3	5,4	14,3	-
	7	48,3	27,3	0,7	3,6	3,1	3,9	12,9	-
	14	48,6	28,7	1	3,9	2,6	3,7	11,5	-
	21	47,7	21,9	2,9	2,7	1,9	6,3	16,6	-
DE:Alg	Time (days)	O	C	Si	Na	Cl	P	Ca	Al
	0	49.8	24.1	16.1	5.8	2.7	1.1	-	-
	1	44,7	21,4	18,8	5,2	6,7	-	2,1	1,1
	3	51,8	20,2	21,1	1,9	1,3	-	2,3	1,4
	7	50,3	21,8	20,5	2,1	2,2	-	2	1,2
	14	49,6	20,9	18,9	2,4	3	-	2,9	1,3
	21	48,8	22,4	20	2,1	3	0,6	2,1	1
GB:Alg	Time (days)	O	C	Si	Na	Cl	P	Ca	Al
	0	46.7	36.4	9.8	0.4	0.9	-	5.8	-
	1	46,7	34,1	9,6	3,7	3,2	-	2,7	-
	3	46,2	34,4	10,7	3,3	2,4	-	3	-
	7	48,1	34,8	7,4	3,5	3,1	-	3,1	-
	14	46	33,8	10,6	3,4	2,8	-	3,2	-
	21	44,9	33	10,3	3,6	4,6	0,5	3,1	-

3.7. Cell culture assays

To check the biocompatibility of the developed scaffolds, we performed a first assessment by evaluation of potential cytotoxicity using SaOS-2 cells. From Figure 10-A, it is noted that COL1 coating improved cell viability in the fabricated scaffolds. A higher concentration of COL1 promoted the higher Alamar Blue Fluorescence. DNA quantification was performed to evaluate cell proliferation in the developed scaffolds. Several differences in the DNA concentration were observed in scaffolds with respective biosilica particles and COL1 coating concentrations. On day 3 of culturing, the BS:Alg scaffolds with 0.5% and 1% COL1 demonstrated a significantly higher amount of DNA when compared with the ones without COL1 coating, as shown in Figure 10-B. The results on DNA quantification are consistent with Alamar Blue Assay indicating improvement of material cytocompatibility by addition of COL1. On day 1 and day 3 after the cell seeding, the GB:Alg scaffolds without coating presented higher DNA concentration when compared to other BS:Alg without coating. Additionally, the GB:Alg + 0.5 COL and GB:Alg + 1% COL presented the higher DNA concentration in comparison to other BS:Alg coated in all time points, excluding the day 3 for scaffold coated with 1 % of COL1.

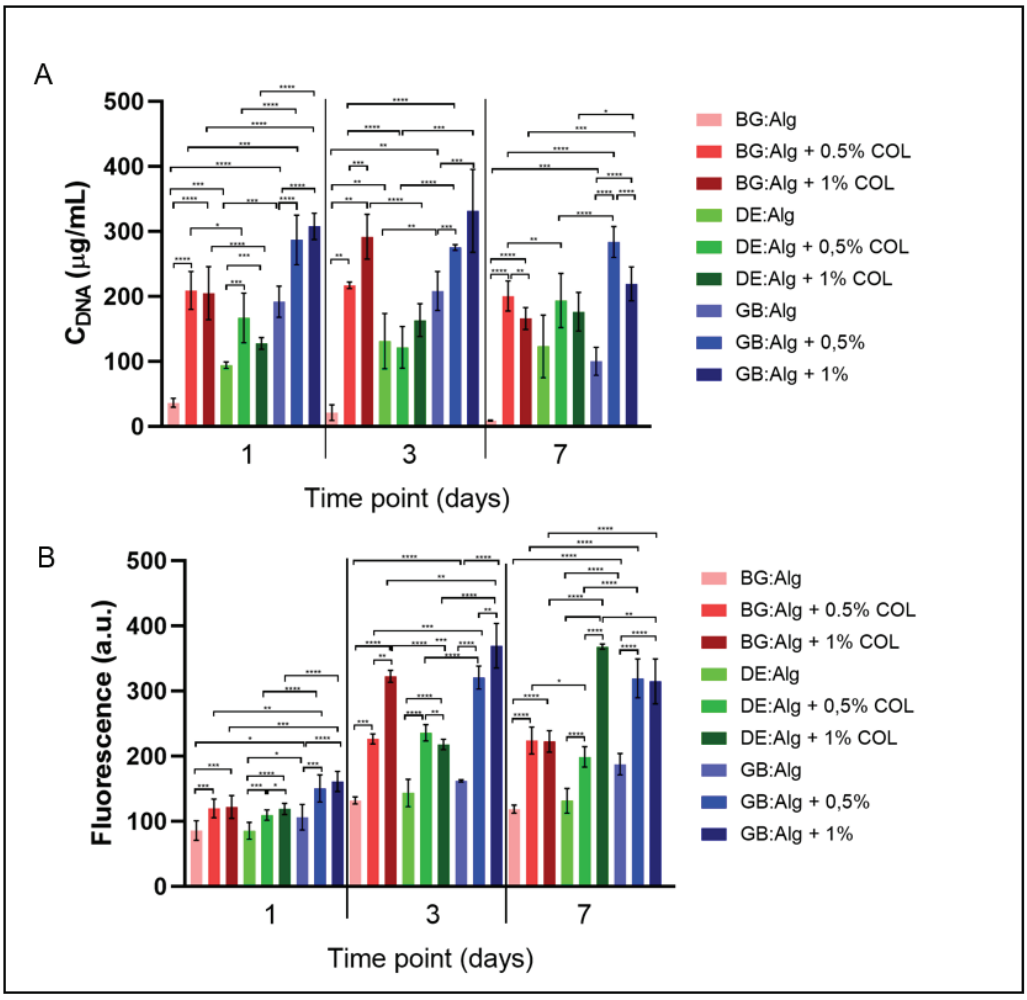

Figure 10. 3D scaffolds' Biological experiments using SaOS-2 cell line culture assay at 1, 3 and 7 days with **A** - DNA quantification, and **B** - Cellular viability. Data in the graphics are presented as mean ± SD and the statistical differences are presented with * for $p < 0.05$, ** for $p < 0.01$, *** for $p < 0.001$ and **** for $p < 0.0001$.

CONCLUSIONS

In this study, biosilica could be retrieved from marine sponge *Geodia barretti* by calcination, and it was tested as a potential bioactive component for preparing printable inks based on alginate hydrogel for 3D printing scaffolds envisaging bone tissue engineering. The effects of GB loading on the mechanical and morphological properties of the resulting scaffolds were evident, with the obtained results showing that the GB:Alg scaffolds presented higher compressive modulus, as well as higher mean pore size and lower total porosity, in comparison to scaffolds comprising other silica-based materials, namely bioglass (BG). The morphological structures of the silica from marine sponge and diatom seems to impact the mechanical resistance of the respective scaffolds. The cytocompatibility of scaffolds were investigated with osteosarcoma cell line and the performance of GB:Alg were favorable to cell attachment and proliferation. Further studies should be performed to observe longer culture periods, but the COL1 also leads to the improvement of the cell attachment, viability and proliferation in all scaffolds. The GB presented interesting properties as bone replacement material's compound. Nevertheless, further studies on the enhancement of scaffold stiffness and bioactivity by incorporation of additional components into the biomaterial ink should be performed.

ACKNOWLEDGMENTS

We acknowledge the financial support from European Union H2020 program through the SponGES project (grant agreement No 679849). The authors would like to thank Dr. Joana R. Xavier from the Interdisciplinary Centre of Marine and Environmental Research, University of Porto, Portugal and from the University of Bergen, Norway, and Prof. Hans Tore Rapp from the University of Bergen, Norway for providing the sponge samples. Sollaris company (Poland) is acknowledged for offering the diatomaceous earth and Mar Lusitano (Gafanha da Nazaré, Portugal) for the kind offer of codfish skins.

REFERENCES

Anderson, J. M. (2016). Future challenges in the in vitro and in vivo evaluation of biomaterial biocompatibility. Regenerative Biomaterials, 3(2), 73-77. Retrieved 9 27, 2021, from https://academic.oup.com/rb/article/3/2/73/2461185

Barros, A. A., Aroso, I. M., Silva, T. H., Mano, J. F., Duarte, A. R., & Reis, R. L. (2014). Surface modification of silica-based marine sponge bioceramics induce hydroxyapatite formation. Crystal Growth & Design, 14(9), 4545-4552. Retrieved 7 4, 2021, from https://pubs.acs.org/doi/10.1021/cg500654u

Bootsma, K., Fitzgerald, M. M., Free, B., Dimbath, E., Conjerti, J., Reese, G. J., . . . Sparks, J. L. (2017). 3D printing of an interpenetrating network hydrogel material with tunable viscoelastic properties. Journal of The Mechanical Behavior of Biomedical Materials, 70, 84-94. Retrieved 9 27, 2021, from https://sciencedirect.com/science/article/pii/s1751616116302363

Dudik, O., Amorim, S., Xavier, J. R., Rapp, H. T., Silva, T. H., Pires, R. A., & Reis, R. L. (2021). Bioactivity of Biosilica Obtained From North Atlantic Deep-Sea Sponges. Frontiers in Marine Science, 8(May), 1–12. https://doi.org/10.3389/fmars.2021.637810

Giannoudis, P. V., Calori, G. M., Bégué, T., & Schmidmaier, G. (2013). Bone regeneration strategies: Current trends but what the future holds? Injury-international Journal of The Care of The Injured, 44. Retrieved 9 27, 2021, from https://ncbi.nlm.nih.gov/pubmed/23351862

Guvendiren, M., Molde, J., Soares, R. M., & Kohn, J. (2016). Designing Biomaterials for 3D Printing. ACS Biomaterials Science & Engineering, 2(10), 1679-1693. Retrieved 9 27, 2021, from https://pubs.acs.org/doi/abs/10.1021/acsbiomaterials.6b00121

Hege, C., & Schiller, S. M. (2015). New Bioinspired Materials for Regenerative Medicine. Retrieved 9 27, 2021, from https://link.springer.com/article/10.1007/s40610-015-0015-1

Hunt, N. C., Shelton, R. M., & Grover, L. M. (2009). AN ALGINATE HYDROGEL MATRIX FOR THE LOCALISED DELIVERY OF A FIBROBLAST/KERATINOCYTE CO-CULTURE. Biotechnology Journal, 4(5), 730-737. Retrieved 9 27, 2021, from https://onlinelibrary.wiley.com/doi/abs/10.1002/biot.200800292

Jakus, A. E., Rutz, A. L., & Shah, R. N. (2016). Advancing the field of 3D biomaterial printing. Biomedical Materials, 11(1), 014102-014102. Retrieved 9 27, 2021, from https://iopscience.iop.org/article/10.1088/1748-6041/11/1/014102/meta

Jones, J. R., Brauer, D. S., Hupa, L., & Greenspan, D. C. (2016). Bioglass and Bioactive Glasses and Their Impact on Healthcare. International Journal of Applied Glass Science, 7(4), 423-434. Retrieved 9 27, 2021, from https://ceramics.onlinelibrary.wiley.com/doi/abs/10.1111/ijag.12252

Kong, Y., Yan, T., Sun, Y., Qian, J., Zhou, G., Cai, S., & Tian, Y. (2019). A dosimetric study on the use of 3D-printed customized boluses in photon therapy: A hydrogel and silica gel study. Journal of Applied Clinical Medical Physics, 20(1), 348-355. Retrieved 9 27, 2021, from https://aapm.onlinelibrary.wiley.com/doi/pdf/10.1002/acm2.12489

Martins, E., Rocha, M. S., Silva, T. H., & Reis, R. L. (2019). Remarkable body architecture of marine sponges as biomimetic structure for application in tissue engineering. In Springer Series in Biomaterials Science and Engineering (Vol. 14). Springer Singapore. https://doi.org/10.1007/978-981-13-8855-2_2

Murata, H. (2012). Rheology - Theory and Application to Biomaterials. Retrieved 9 27, 2021, from https://intechopen.com/books/polymerization/rheology-theory-and-application-to-biomaterials

Sargus-Patino, C. (2013). Alginate Hydrogel as a Three-dimensional Extracellular Matrix for In Vitro Models of Development. Retrieved 8 13, 2021, from https://digitalcommons.unl.edu/cgi/viewcontent.cgi?article=1037&context=biosysengdiss

Soni, R., Roopavath, U. K., Mahanta, U., Deshpande, A. S., & Rath, S. N. (2018). Sodium alginate/gelatin with silica nanoparticles is a novel hydrogel for 3D printing. Retrieved 9 27, 2021, from https://ui.adsabs.harvard.edu/abs/2018aipc.1966b0002s/abstract

Tan, Y., Tan, Y., Richards, D. J., Richards, D. J., Trusk, T. C., Visconti, R. P., . . . Mei, Y. (2014). 3D Printing Facilitated Scaffold-free Tissue Unit Fabrication. Biofabrication, 6(2), 024111-024111. Retrieved 9 27, 2021, from https://ncbi.nlm.nih.gov/pubmed/24717646

Zhang, L., Yang, G., Johnson, B. N., & Jia, X. (2019). Three-dimensional (3D) Printed Scaffold and Material Selection for Bone Repair. Acta Biomaterialia, 84, 16-33. Retrieved 9 27, 2021, from https://sciencedirect.com/science/article/pii/s1742706118307025

CONCLUSION AND FUTURE PERSPECTIVES

Our main objective in this work was successfully attended by the evaluation of the sponge-derived biosilica as potential component of biomaterials for bone tissue engineering, namely 3D printing scaffolds, in comparison to other silica-based materials - Diatomaceous earth and Bioglass 45S5®. Biosilica could be retrieved from marine sponge *Geodia barretti* by calcination at 600 °C, which was required for the elimination of organic matter but also caused the fracture of the biosilica spicules. Alternative procedures for the isolation of sponge spicules can be tested in the future, namely the processing of sponge samples with nitric acid, to access if the partial fracture of the spicules has influence on the elaboration of inks and the consequent performance of the 3D printed scaffolds.

It was possible to develop ink formulations based on biosilica, after adjusting the conditions for ion gelation of alginate that enable the production of a printable hydrogel. This was performed by considering the amount of added calcium chloride and the ratio of alginate and biosilica, considering that the initial concentration of alginate has been determined in previous studies. The 3D-printed scaffolds produced with the developed protocol using the three types of silica-based materials presented a similar morphological profile, with similar interconnectivity and porosity, with an exception for the mean pore size of BG:Alg, which may be by working on the definitions of the design model established for printing. Playing with the morphological characteristics of the scaffolds may enable to improve the mechanical resistance of the scaffolds to compression, aiming to achieve the minimum necessary to be used as a replacement component for cancellous bone, while the current design resulted in compressive moduli significantly lower than the reference values for bone, thus suggesting the use of the developed scaffolds for non-load-bearing applications only.

The scaffolds developed with biosilica derived from *Geodia barretti* presented interesting performance on the *in vitro* biological pilot experiment, exhibiting higher DNA amount (proportional to the number of cells) than the one observed with scaffolds produced with bioglass. However, during the culture time studied (7 days), it was not possible to observe a clear cell proliferation, despite the apparent increment in cell metabolic activity (used to assess cell viability). This may suggest that seeded cells are still adapting to the template matrix and eventually proliferation could be observed with longer culture times. In this regard, it is also recommended to perform microscopic analysis of the cell-laden scaffolds at different culture times to better assess cell adhesion, spatial distribution and morphology in these scaffolds.

The marine biosilica presented a interesting potential for bone tissue engineering from the chemical composition of these organisms and *Geodia barretti,* as observed in our study has physico-chemical and morphological properties that deserves special attention as a candidate for biomaterial applications in further studies as a bioceramic for bone tissue engineering. The bioactivity may be performed in association with a technique to evaluate the composition of the elements dissolved in water. The biodegradability assay may be performed as well, to evaluate the silica-based particles in comparison to biopolymer degradation.

BIBLIOGRAPHY

Abdelmohsen, U. R., Abdelmohsen, U. R., Bayer, K., & Hentschel, U. (2014). Diversity, abundance and natural products of marine sponge-associated actinomycetes. Natural Product Reports, 31(3), 381-399. Retrieved 9 23, 2021, from http://oceanrep.geomar.de/29119

Akhir, H. M., & Teoh, P. L. (2020). Collagen type I promotes osteogenic differentiation of amniotic membrane-derived mesenchymal stromal cells in basal and induction media. Bioscience Reports, 40(12), 1–12. https://doi.org/10.1042/BSR20201325

Anderson, J. M. (2016). Future challenges in the in vitro and in vivo evaluation of biomaterial biocompatibility. Regenerative Biomaterials, 3(2), 73-77. Retrieved 9 27, 2021, from https://academic.oup.com/rb/article/3/2/73/2461185

Augst, A., Kong, H., & Mooney, D. J. (2006). Alginate Hydrogels as Biomaterials. Macromolecular Bioscience, 6(8), 623-633. Retrieved 8 13, 2021, from https://onlinelibrary.wiley.com/doi/abs/10.1002/mabi.200600069

Barros, A. A., Aroso, I. M., Silva, T. H., Mano, J. F., Duarte, A. R., & Reis, R. L. (2014). Surface modification of silica-based marine sponge bioceramics induce hydroxyapatite formation. Crystal Growth & Design, 14(9), 4545-4552. Retrieved 7 4, 2021, from https://pubs.acs.org/doi/10.1021/cg500654u

Barros, A. A., Aroso, I. M., Silva, T. H., Mano, J. F., Duarte, A. R., & Reis, R. L. (2016). In vitro bioactivity studies of ceramic structures isolated from marine sponges. Biomedical Materials, 11(4), 045004-045004. Retrieved 4 28, 2021, from http://iopscience.iop.org/article/10.1088/1748-6041/11/4/045004/pdf

Bose, S., Vahabzadeh, S., & Bandyopadhyay, A. (2013). Bone tissue engineering using 3D printing. Materials Today, 16(12), 496-504. Retrieved 8 13, 2021, from https://sciencedirect.com/science/article/pii/s136970211300401x

Bootsma, K., Fitzgerald, M. M., Free, B., Dimbath, E., Conjerti, J., Reese, G. J., . . . Sparks, J. L. (2017). 3D printing of an interpenetrating network hydrogel material with tunable viscoelastic properties. Journal of The Mechanical Behavior of Biomedical Materials, 70, 84-94. Retrieved 9 27, 2021, from https://sciencedirect.com/science/article/pii/s1751616116302363

Buonocore, F. (2012). Marine Biotechnology: Developments and Perspectives. Journal of Aquaculture Research and Development, 04(02). Retrieved 9 23, 2021, from https://omicsonline.org/marine-biotechnology-developments-and-perspectives-2155-9546.1000e105.pdf

Cárdenas, P., & Rapp, H. T. (2015). Demosponges from the Northern Mid-Atlantic Ridge shed more light on the diversity and biogeography of North Atlantic deep-sea sponges. Journal of the Marine Biological Association of the United Kingdom, 95(7), 1475–1516. https://doi.org/10.1017/S0025315415000983

Cassarino, L., Coath, C. D., Xavier, J. R., & Hendry, K. R. (2018). Silicon isotopes of deep-sea sponges: new insights into biomineralisation and skeletal structure. Biogeosciences, 15(22), 6959-6977. Retrieved 8 13, 2021, from https://biogeosciences.net/15/6959/2018/bg-15-6959-2018.pdf

Catherine, H., & Skinner, W. (2000). Minerals and human health. In D. J. Vaughan & R. A. Wogelius (Eds.), Environmental Mineralogy (Vol. 2, p. 0). Mineralogical Society of Great Britain and Ireland. https://doi.org/10.1180/EMU-notes.2.11

Chen, Q., Zhu, C., & Thouas, G. A. (2012). Progress and challenges in biomaterials used for bone tissue engineering: bioactive glasses and elastomeric composites. Progress in

Biomaterials, 1(1), 1-22. Retrieved 8 13, 2021, from https://link.springer.com/article/10.1186/2194-0517-1-2

Chia, H. N., & Wu, B. M. (2015). Recent advances in 3D printing of biomaterials. Journal of Biological Engineering, 9(1), 4-4. Retrieved 4 27, 2021, from https://jbioleng.biomedcentral.com/articles/10.1186/s13036-015-0001-4

Chia, H. N., Wu, G., Weiss, T. L., Gu, B. K., Wardyn, J. D., & Dombroski, C. E. (2016). 3D Printing in Medicine. Retrieved 4 27, 2021, from https://scirp.org/book/detailedinforofabook.aspx?bookid=2374

Chiu, L. H., Lai, W. F. T., Chang, S. F., Wong, C. C., Fan, C. Y., Fang, C. L., & Tsai, Y. H. (2014). The effect of type II collagen on MSC osteogenic differentiation and bone defect repair. Biomaterials, 35(9), 2680–2691. https://doi.org/10.1016/j.biomaterials.2013.12.005

Cl, V. (2014). Medical Applications for 3D Printing: Current and Projected Uses. P & T : a peer-reviewed journal for formulary management, 39(10), 704-711. Retrieved 4 27, 2021, from https://ncbi.nlm.nih.gov/pmc/articles/pmc4189697

D, K. D. (2020). Biosilica : Structure, function, science, technology and inspiration. 103(February), 1009–1010.

Demadis, K. D. (2018). Biosilica: Structure, function, science, technology, and inspiration. American Mineralogist, 103(7), 1009-1010. Retrieved 4 27, 2021, from https://pubs.geoscienceworld.org/msa/ammin/article/103/7/1009/537194/biosilica-structure-function-science-technology

Donati, I., & Paoletti, S. (2009). Material Properties of Alginates. Retrieved 8 13, 2021, from https://link.springer.com/chapter/10.1007/978-3-540-92679-5_1

Douglas, T. (2016). Biomimetic mineralization of hydrogels. Retrieved 4 27, 2021, from https://sciencedirect.com/science/article/pii/b9781782423386000107

Dudik, O., Amorim, S., Xavier, J. R., Rapp, H. T., Silva, T. H., Pires, R. A., & Reis, R. L. (2021). Bioactivity of Biosilica Obtained from North Atlantic Deep-Sea Sponges. Frontiers in Marine Science, 8(May), 1–12. https://doi.org/10.3389/fmars.2021.637810

Gabbai-Armelin, P. R., Kido, H. W., Cruz, M. A., Prado, J. P., Avanzi, I. R., Custódio, M. R., . . . Granito, R. N. (2019). Characterization and Cytotoxicity Evaluation of a Marine Sponge Biosilica. Marine Biotechnology, 21(1), 65-75. Retrieved 8 13, 2021, from https://link.springer.com/article/10.1007/s10126-018-9858-9

Ghorbani, F., Li, D., Ni, S., Zhou, Y., & Yu, B. (2020). 3D printing of acellular scaffolds for bone defect regeneration: A review. Materials Today Communications, 22(January). https://doi.org/10.1016/j.mtcomm.2020.100979

Greenwald, A. S., Boden, S. D., Goldberg, V. M., Khan, Y., Laurencin, C. T., & Rosier, R. N. (2001). Bone-graft Substitutes: Facts, Fictions, and Applications. Journal of Bone and Joint Surgery, American Volume, 83, 98-103. Retrieved 8 4, 2021, from https://ncbi.nlm.nih.gov/pubmed/11712842

Groll, J., Boland, T., Blunk, T., Burdick, J. A., Cho, D. W., Dalton, P. D., Derby, B., Forgacs, G., Li, Q., Mironov, V. A., Moroni, L., Nakamura, M., Shu, W., Takeuchi, S., Vozzi, G., Woodfield, T. B. F., Xu, T., Yoo, J. J., & Malda, J. (2016). Biofabrication: Reappraising the definition of an evolving field. Biofabrication, 8(1). https://doi.org/10.1088/1758-5090/8/1/013001

Guvendiren, M., Molde, J., Soares, R. M., & Kohn, J. (2016). Designing Biomaterials for 3D Printing. ACS Biomaterials Science & Engineering, 2(10), 1679-1693. Retrieved 9 27, 2021, from https://pubs.acs.org/doi/abs/10.1021/acsbiomaterials.6b00121

Han, R., Buchanan, F., Julius, M., & Walsh, P. (2017). The investigation of marine derived biosilica for bone repair strategies. Retrieved 4 27, 2021, from https://pure.qub.ac.uk/en/publications/the-investigation-of-marine-derived-biosilica-for-bone-repair-str

Hardoim, C. C., & Costa, R. (2014). Microbial Communities and Bioactive Compounds in Marine Sponges of the Family Irciniidae—A Review. Marine Drugs, 12(10), 5089-5122. Retrieved 8 13, 2021, from https://mdpi.com/1660-3397/12/10/5089/htm

Hege, C., & Schiller, S. M. (2015). New Bioinspired Materials for Regenerative Medicine. Retrieved 9 27, 2021, from https://link.springer.com/article/10.1007/s40610-015-0015-1

Hunt, N. C., Shelton, R. M., & Grover, L. M. (2009). AN ALGINATE HYDROGEL MATRIX FOR THE LOCALISED DELIVERY OF A FIBROBLAST/KERATINOCYTE CO-CULTURE. Biotechnology Journal, 4(5), 730-737. Retrieved 9 27, 2021, from https://onlinelibrary.wiley.com/doi/abs/10.1002/biot.200800292

Jakus, A. E., Rutz, A. L., & Shah, R. N. (2016). Advancing the field of 3D biomaterial printing. Biomedical Materials, 11(1), 014102-014102. Retrieved 9 27, 2021, from https://iopscience.iop.org/article/10.1088/1748-6041/11/1/014102/meta

Jensen, P. R., & Moore, B. S. (2010). Biomedical Development of New Marine Microbial Resources. California Sea Grant College Program. Retrieved 4 27, 2021, from https://escholarship.org/uc/item/41g0k84v

Jones, J. R., Brauer, D. S., Hupa, L., & Greenspan, D. C. (2016). Bioglass and Bioactive Glasses and Their Impact on Healthcare. International Journal of Applied Glass Science, 7(4), 423-434. Retrieved 9 27, 2021, from https://ceramics.onlinelibrary.wiley.com/doi/abs/10.1111/ijag.12252

Kampleitner, C., Obi, J., Vassilev, N., Epstein, M. M., & Hoffmann, O. (2018). Biological Compatibility Profile on Biomaterials for Bone Regeneration. Journal of Visualized Experiments(141). Retrieved 9 16, 2021, from https://jove.com/video/58077/biological-compatibility-profile-on-biomaterials-for-bone-regeneration

Keaveny, T. M., Morgan, E. F., Niebur, G. L., & Yeh, O. C. (2001). Biomechanics of.

Khan, Y., Yaszemski, M. J., Mikos, A. G., & Laurencin, C. T. (2008). Tissue engineering of bone: material and matrix considerations. Journal of Bone and Joint Surgery, American Volume, 90, 36-42. Retrieved 9 23, 2021, from https://ncbi.nlm.nih.gov/pubmed/18292355

Kim, G. (2015). Mineralized biomimetic collagen/alginate/silica composite scaffolds for tissue engineering. Journal of Biomimetics, Biomaterials, and Tissue Engineering. Retrieved 4 28, 2021, from https://omicsonline.org/proceedings/mineralized-biomimetic-collagenalginatesilica-composite-scaffolds-for-tissue-engineering-29751.html

Kim, Y., & Kim, G. (2013). Collagen/alginate scaffolds comprising core (PCL)–shell (collagen/alginate) struts for hard tissue regeneration: fabrication, characterisation, and cellular activities. Journal of Materials Chemistry B, 1(25), 3185-3194. Retrieved 4 28, 2021, from https://pubs.rsc.org/en/content/articlelanding/2013/tb/c3tb20485e#!

King, O. H. (1995). Estimating the value of marine resources: a marine recreation case. Ocean & Coastal Management, 27, 129-141. Retrieved 4 27, 2021, from http://appstate.edu/~whiteheadjc/eco3620/projects/mocktrial/pdf/king-ocm.pdf

Klitgaard, A. B., & Tendal, O. S. (2004). Distribution and species composition of mass occurrences of large-sized sponges in the northeast Atlantic. Progress in Oceanography, 61(1), 57–98. https://doi.org/10.1016/j.pocean.2004.06.002

Kokubo, T., Kushitani, H., Sakka, S., Kitsugi, T., & Yamamuro, T. (1990). Solutions able to reproduce in vivo surface-structure changes in bioactive glass-ceramic A-W3. Journal of

Biomedical Materials Research, 24(6), 721-734. Retrieved 8 12, 2021, from https://onlinelibrary.wiley.com/doi/abs/10.1002/jbm.820240607

Lee, H., Ahn, S., & Kim, G. (2012). Three-Dimensional Collagen/Alginate Hybrid Scaffolds Functionalized with a Drug Delivery System (DDS) for Bone Tissue Regeneration. Chemistry of Materials, 24(5), 881-891. Retrieved 4 28, 2021, from https://pubs.acs.org/doi/10.1021/cm200733s

Ma, P. X. (2008). Biomimetic materials for tissue engineering. Advanced Drug Delivery Reviews, 60(2), 184-198. Retrieved 8 13, 2021, from https://ncbi.nlm.nih.gov/pmc/articles/pmc2271038

Martins, E., Rocha, M. S., Silva, T. H., & Reis, R. L. (2019). Remarkable body architecture of marine sponges as biomimetic structure for application in tissue engineering. In Springer Series in Biomaterials Science and Engineering (Vol. 14). Springer Singapore. https://doi.org/10.1007/978-981-13-8855-2_2

Mistry, P. (2018). Development of a core-shell composite hydrogel for 3D bioprinting. Retrieved 8 13, 2021, from http://eprints.nottingham.ac.uk/50395

Müller, W. E., Albert, O., Schröder, H. C., & Wang, X. H. (2014). Bio-inorganic Nanomaterials for Biomedical Applications (Bio-silica and Polyphosphate). Retrieved 8 13, 2021, from https://link.springer.com/chapter/10.1007/978-3-642-31107-9_22

Müller, W. E., Schloßmacher, U., Eckert, C., Krasko, A., Boreiko, A., Ushijima, H., . . . Schröder, H. C. (2007). Analysis of the axial filament in spicules of the demosponge Geodia cydonium: Different silicatein composition in microscleres (asters) and megascleres (oxeas and triaenes). European Journal of Cell Biology, 86(8), 473-487. Retrieved 8 13, 2021, from https://sciencedirect.com/science/article/pii/s0171933507000799

Murali, P., Ramamurty, U., & Shenoy, V. B. (2008). Factors influencing deformation stability of binary glasses. Journal of Chemical Physics, 128(10), 104508-104508. Retrieved 4 28, 2021, from http://materials.iisc.ernet.in/~ramu/publications/paper68.pdf

Murata, H. (2012). Rheology - Theory and Application to Biomaterials. Retrieved 9 27, 2021, from https://intechopen.com/books/polymerization/rheology-theory-and-application-to-biomaterials

Nandi, S. K., Kundu, B., Mahato, A., Thakur, N. L., Joardar, S. N., & Mandal, B. B. (2015). In vitro and in vivo evaluation of the marine sponge skeleton as a bone mimicking biomaterial. Integrative Biology, 7(2), 250-262. Retrieved 9 23, 2021, from https://ncbi.nlm.nih.gov/pubmed/25578396

Neves, N. M., Pouzada, A. S., Voerman, J., & Powell, P. (1998). The use of birefringence for predicting the stiffness of injection molded polycarbonate discs. Polymer Engineering and Science, 38(10), 1770-1777. Retrieved 4 28, 2021, from http://onlinelibrary.wiley.com/doi/10.1002/pen.10347/abstract

Nguyen, L. H., Nguyen, L. H., Annabi, N., Annabi, N., Nikkhah, M., Bae, H., . . . Khademhosseini, A. (2012). Vascularized Bone Tissue Engineering: Approaches for Potential Improvement. Tissue Engineering Part B-reviews, 18(5), 363-382. Retrieved 8 13, 2021, from https://ncbi.nlm.nih.gov/pmc/articles/pmc3458624

Nowak, A., Sprynskyy, M., Brzozowska, W., & Lisowska-Oleksiak, A. (2019). Electrochemical behavior of a composite material containing 3D-structured diatom biosilica. Algal Research-Biomass Biofuels and Bioproducts, 41, 101538. Retrieved 4 27, 2021, from https://sciencedirect.com/science/article/pii/s2211926419301882

Patients, S., in Solid Cancer, P. C., Hassan, B. A. R., Yusoff, Z. B. M., Othman, M. A. H., Bin, S., information is available at the end of the Chapter, A., &

Http://dx.doi.org/10.5772/55358. (2012). We are IntechOpen, the world's leading publisher of Open Access books Built by scientists, for scientists TOP 1 %. Intech, tourism, 13.

Pugliese, R., Beltrami, B., Regondi, S., & Lunetta, C. (2021). Polymeric biomaterials for 3D printing in medicine: An overview. Annals of 3D Printed Medicine, 2, 100011. https://doi.org/10.1016/j.stlm.2021.100011

Roberts, T. T., & Rosenbaum, A. J. (2012). Bone grafts, bone substitutes and orthobiologics: The bridge between basic science and clinical advancements in fracture healing. Organogenesis, 8(4), 114-124. Retrieved 8 4, 2021, from https://ncbi.nlm.nih.gov/pmc/articles/pmc3562252

Rowley, J. A., Madlambayan, G., & Mooney, D. J. (1999). Alginate hydrogels as synthetic extracellular matrix materials. Biomaterials, 20(1), 45-53. Retrieved 8 13, 2021, from https://sciencedirect.com/science/article/pii/s0142961298001070

Sabdono, A., & Radjasa, O. K. (2011). MICROBIAL SYMBIONTS IN MARINE SPONGES: Marine natural product factory. Journal of Coastal Zone Management, 11(2), 57-61. Retrieved 9 23, 2021, from https://longdom.org/open-access/microbial-symbionts-in-marine-sponges-marine-natural-product-factory-1410-5217-11-239.pdf

Sagar, S., Kaur, M., & Minneman, K. P. (2010). Antiviral Lead Compounds from Marine Sponges. Marine Drugs, 8(10), 2619-2638. Retrieved 8 13, 2021, from https://ncbi.nlm.nih.gov/pmc/articles/pmc2992996

Sagar, S., Kaur, M., Radovanovic, A., & Bajic, V. B. (2013). Dragon exploration system on marine sponge compounds interactions. Journal of Cheminformatics, 5(1), 11-11. Retrieved 9 23, 2021, from https://jcheminf.biomedcentral.com/track/pdf/10.1186/1758-2946-5-11

Sahranavard, M., Zamanian, A., Ghorbani, F., & Shahrezaee, M. H. (2020). A critical review on three-dimensional-printed chitosan hydrogels for development of tissue engineering. Bioprinting, 17, e00063. https://doi.org/10.1016/j.bprint.2019.e00063

Sargus-Patino, C. (2013). Alginate Hydrogel as a Three-dimensional Extracellular Matrix for In Vitro Models of Development. Retrieved 8 13, 2021, from https://digitalcommons.unl.edu/cgi/viewcontent.cgi?article=1037&context=biosysengdiss

Sarker, B., Singh, R. P., Silva, R., Roether, J. A., Kaschta, J., Detsch, R., . . . Boccaccini, A. R. (2014). Evaluation of Fibroblasts Adhesion and Proliferation on Alginate-Gelatin Crosslinked Hydrogel. PLOS ONE, 9(9). Retrieved 8 13, 2021, from https://journals.plos.org/plosone/article?id=10.1371/journal.pone.0107952

Schröder, H. C., Brandt, D., Schloßmacher, U., Wang, X., Tahir, M. N., Tremel, W., . . . Müller, W. E. (2007). Enzymatic production of biosilica glass using enzymes from sponges: basic aspects and application in nanobiotechnology (material sciences and medicine). Naturwissenschaften, 94(5), 339-359. Retrieved 4 27, 2021, from https://link.springer.com/article/10.1007/s00114-006-0192-0

Schröder, H. C., Wiens, M., Wang, X., Schloßmacher, U., & Müller, W. E. (2011). Biosilica-Based Strategies for Treatment of Osteoporosis and Other Bone Diseases. Progress in molecular and subcellular biology, 52, 283-312. Retrieved 8 13, 2021, from https://link.springer.com/chapter/10.1007/978-3-642-21230-7_10

Shafiee, A., & Atala, A. (2016). Printing Technologies for Medical Applications. Trends in Molecular Medicine, 22(3), 254-265. Retrieved 8 13, 2021, from https://sciencedirect.com/science/article/abs/pii/s1471491416000149

Shegarfi, H., & Reikeras, O. (2009). Review article: bone transplantation and immune response. Journal of Orthopaedic Surgery (Hong Kong), 17(2), 206–211. https://doi.org/10.1177/230949900901700218

Sheikh, Z., Najeeb, S., Khurshid, Z., Verma, V., Rashid, H., & Glogauer, M. (2015). Biodegradable materials for bone repair and tissue engineering applications. Materials, 8(9), 5744–5794. https://doi.org/10.3390/ma8095273

Silva, S. S., Oliveira, M. B., Mano, J. F., & Reis, R. L. (2014). Bio-inspired Aloe vera sponges for biomedical applications. Carbohydrate Polymers, 112, 264-270. Retrieved 8 13, 2021, from https://sciencedirect.com/science/article/pii/s0144861714005128

Silva, T. H., Alves, A., Ferreira, B. M., Oliveira, J. M., Reys, L. L., Ferreira, R. J., . . . Reis, R. L. (2012). Materials of marine origin: a review on polymers and ceramics of biomedical interest. International Materials Reviews, 57(5), 276-306. Retrieved 4 27, 2021, from http://repositorium.sdum.uminho.pt/bitstream/1822/21720/1/imr200.pdf

Silva, T. H., Moreira-Silva, J., Marques, A. L., Domingues, A., Bayon, Y., & Reis, R. L. (2014). Marine Origin Collagens and Its Potential Applications. Marine Drugs, 12(12), 5881-5901. Retrieved 9 23, 2021, from https://ncbi.nlm.nih.gov/pmc/articles/pmc4278207

Sinha, S. K. (2020). Additive manufacturing (AM) of medical devices and scaffolds for tissue engineering based on 3D and 4D printing. Retrieved 8 13, 2021, from https://sciencedirect.com/science/article/pii/b9780128168059000053

Smith, I. O., & Ma, P. X. (2011). Biomimetic scaffolds in tissue engineering. Retrieved 8 13, 2021, from https://link.springer.com/chapter/10.1007/978-3-642-02824-3_2

Solaris, P.-G. I. (2021, May 04). Perma Guard Europe. Retrieved from Perma Guard Europe: https://www.pgsilica.com/okrzemki-diatomit/

Sousa, R. O., Martins, E., Carvalho, D. N., Alves, A. L., Oliveira, C., Duarte, A. R. C., Silva, T. H., & Reis, R. L. (2020). Collagen from Atlantic cod (Gadus morhua) skins extracted using CO2 acidified water with potential application in healthcare. Journal of Polymer Research, 27(3). https://doi.org/10.1007/s10965-020-02048-x

Sprio, S., Sandri, M., Panseri, S., Iafisco, M., Ruffini, A., Minardi, S., & Tampieri, A. (2014). Bone substitutes based on biomineralization. In Bone Substitute Biomaterials. Woodhead Publishing Limited. https://doi.org/10.1533/9780857099037.1.3

Stein, E. M., Ebeling, P. R., & Shane, E. (2007). Post-Transplantation Osteoporosis. Endocrinology and Metabolism Clinics of North America, 36(4), 937-963. Retrieved 8 4, 2021, from https://ncbi.nlm.nih.gov/pubmed/17983930

Tamburaci, S., & Tihminlioglu, F. (2018). Biosilica incorporated 3D porous scaffolds for bone tissue engineering applications. Materials Science and Engineering C, 91(May), 274–291. https://doi.org/10.1016/j.msec.2018.05.040

Tan, Y., Tan, Y., Richards, D. J., Richards, D. J., Trusk, T. C., Visconti, R. P., . . . Mei, Y. (2014). 3D Printing Facilitated Scaffold-free Tissue Unit Fabrication. Biofabrication, 6(2), 024111-024111. Retrieved 9 27, 2021, from https://ncbi.nlm.nih.gov/pubmed/24717646

Valisano, L., Pozzolini, M., Giovine, M., & Cerrano, C. (2012). Biosilica deposition in the marine sponge Petrosia ficiformis (Poiret, 1789): the model of primmorphs reveals time dependence of spiculogenesis. Hydrobiologia, 687(1), 259-273. Retrieved 4 27, 2021, from https://link.springer.com/article/10.1007/s10750-011-0987-7

Venkatesan, J., Anil, S., Chalisserry, E. P., & Kim, S.-K. (2016). Marine Sponges as Future Biomedical Models. Retrieved 8 13, 2021, from https://link.springer.com/chapter/10.1007/978-81-322-2794-6_18

Venkatesan, J., Bhatnagar, I., Manivasagan, P., Kang, K.-H., & Kim, S.-K. (2015). Alginate composites for bone tissue engineering: A review. International Journal of Biological Macromolecules, 72, 269-281. Retrieved 4 27, 2021, from https://sciencedirect.com/science/article/pii/s0141813014004735

Visser, J., Melchels, F. P., Dhert, W. J., & Malda, J. (2013). [Tissue printing; the potential application of 3D printing in medicine]. Nederlands Tijdschrift voor Geneeskunde, 157(52). Retrieved 4 27, 2021, from https://ncbi.nlm.nih.gov/pubmed/24382049

Vogl, F., Bernet, B., Bolognesi, D., & Taylor, W. R. (2017). Towards assessing cortical bone porosity using low-frequency quantitative acoustics: A phantom-based study. PLoS ONE, 12(9), 1–14. https://doi.org/10.1371/journal.pone.0182617

Walls, H. J., Caines, S. B., Sanchez, A. M., & Khan, S. A. (2003). Yield stress and wall slip phenomena in colloidal silica gels. Journal of Rheology, 47(4), 847–868. https://doi.org/10.1122/1.1574023

Walsh, P., Clarke, S., Julius, M. L., Buchanan, F., & Messersmith, P. B. (2015). Marine Biosilica as a Tool to Understand the Therapeutic Benefit of Silica in Bone Repair. Retrieved 4 27, 2021, from https://pure.qub.ac.uk/en/publications/marine-biosilica-as-a-tool-to-understand-the-therapeutic-benefit-

Walsh, P., Clarke, S., Strehin, I., Messersmith, P., & Messersmith, P. (2014). Marine inspired biosilica-filled hydrogels for hard tissue repair. Retrieved 4 27, 2021, from https://pure.qub.ac.uk/portal/en/publications/marine-inspired-biosilicafilled-hydrogels-for-hard-tissue-repair(12758dbc-826f-49b2-bee6-c980a0e0e70b).html

Wang, X., Schröder, H. C., Grebenjuk, V. A., Diehl-Seifert, B., Mailänder, V., Steffen, R., . . . Müller, W. E. (2014). The marine sponge-derived inorganic polymers, biosilica and polyphosphate, as morphogenetically active matrices/scaffolds for the differentiation of human multipotent stromal cells: potential application in 3D printing and distraction osteogenesis. Marine Drugs, 12(2), 1131-1147. Retrieved 4 27, 2021, from https://mdpi.com/1660-3397/12/2/1131/pdf

Wang, X., Tolba, E., Schröder, H. C., Neufurth, M., Feng, Q., Diehl-Seifert, B., & Müller, W. E. (2014). Effect of Bioglass on Growth and Biomineralization of SaOS-2 Cells in Hydrogel after 3D Cell Bioprinting. PLOS ONE, 9(11). Retrieved 4 27, 2021, from https://journals.plos.org/plosone/article?id=10.1371/journal.pone.0112497

Wang, X., Xu, S., Zhou, S., Xu, W., Leary, M., Choong, P., Qian, M., Brandt, M., & Xie, Y. M. (2016). Topological design and additive manufacturing of porous metals for bone scaffolds and orthopedic implants: A review. Biomaterials, 83, 127–141. https://doi.org/10.1016/j.biomaterials.2016.01.012

Weisinger, J. R., Carlini, R. G., Rojas, E., & Bellorin-Font, E. (2006). Bone disease after renal transplantation. Clinical Journal of The American Society of Nephrology, 1(6), 1300-1313. Retrieved 8 4, 2021, from https://cjasn.asnjournals.org/content/1/6/1300

Wetherbee, R., Crawford, S., & Mulvaney, P. (2005). The Nanostructure and Development of Diatom Biosilica. Retrieved 4 27, 2021, from https://findanexpert.unimelb.edu.au/scholarlywork/1030195-the-nanostructure-and-development-of-diatom-biosilica

Wiens, M., Wang, X., Natalio, F., Schröder, H. C., Schloßmacher, U., Wang, S., . . . Müller, W. E. (2010). Bioinspired Fabrication of Bio-Silica-Based Bone-Substitution Materials. Advanced Engineering Materials, 12(9). Retrieved 8 13, 2021, from https://onlinelibrary.wiley.com/doi/pdf/10.1002/adem.200980043

Williams, A., & Szabo, R. M. (2004). Bone transplantation. Orthopedics, 27(5), 488–495. https://doi.org/10.3928/0147-7447-20040501-17

Woesz, A., Weaver, J. C., Kazanci, M., Dauphin, Y., Aizenberg, J., Morse, D. E., & Fratzl, P. (2006). Micromechanical properties of biological silica in skeletons of deep-sea sponges. Journal of Materials Research, 21(8), 2068-2078. Retrieved 8 13, 2021, from https://cambridge.org/core/journals/journal-of-materials-research/article/micromechanical-

properties-of-biological-silica-in-skeletons-of-deep-sea-sponges/ae7f5af80cff5bb80973f79f8adaf3fe

Wu, Z., Su, X., Xu, Y., Kong, B., Sun, W., Sun, W., & Mi, S. (2016). Bioprinting three-dimensional cell-laden tissue constructs with controllable degradation. Scientific Reports, 6(1), 24474-24474. Retrieved 8 13, 2021, from https://nature.com/articles/srep24474

Wulff, J. L. (2012). Ecological Interactions and the Distribution, Abundance, and Diversity of Sponges. Advances in Marine Biology, 61, 273-344. Retrieved 8 13, 2021, from https://sciencedirect.com/science/article/pii/b9780123877871000039

Zamani, D., Moztarzadeh, F., & Bizari, D. (2019). Alginate-bioactive glass containing Zn and Mg composite scaffolds for bone tissue engineering. International Journal of Biological Macromolecules, 137, 1256-1267. Retrieved 4 27, 2021, from https://sciencedirect.com/science/article/pii/s0141813019300194